DESIGN, CONTROL AND MOTION PLANNING FOR A NOVEL MODULAR EXTENDABLE ROBOTIC MANIPULATOR

A Dissertation

by

HAK YI

Submitted to the Office of Graduate Studies of
Texas A&M University
in partial fulfillment of the requirements for the degree of

DOCTOR OF PHILOSOPHY

Approved by:

Chair of Committee,	Reza Langari
Committee Members,	Richard Malak
	Sivakumar Rathinam
	Dylan Shell
Head of Department,	Jerald A. Caton

December 2012

Major Subject: Mechanical Engineering

ABSTRACT

This dissertation discusses an implementation of a design, control and motion planning for a novel extendable modular redundant robotic manipulator in space constraints, which robots may encounter for completing required tasks in small and constrained environment.

The design intent is to facilitate the movement of the proposed robotic manipulator in constrained environments, such as rubble piles. The proposed robotic manipulator with multi Degree of Freedom (m-DOF) links is capable of elongating by 25% of its nominal length. In this context, a design optimization problem with multiple objectives is also considered. In order to identify the benefits of the proposed design strategy, the reachable workspace of the proposed manipulator is compared with that of the Jet Propulsion Laboratory (JPL) serpentine robot. The simulation results show that the proposed manipulator has a relatively efficient reachable workspace, needed in constrained environments. The singularity and manipulability of the designed manipulator are investigated. In this study, we investigate the number of links that produces the optimal design architecture of the proposed robotic manipulator. The total number of links decided by a design optimization can be useful distinction in practice

Also, we have considered a novel robust bio-inspired Sliding Mode Control (SMC) to achieve favorable tracking performance for a class of robotic manipulators with uncertainties. To eliminate the chattering problem of the conventional sliding mode control, we apply the Brain Emotional Learning Based Intelligent Control (BELBIC) to

adaptively adjust the control input law in sliding mode control. The on-line computed parameters achieve favorable system robustness in process of parameter uncertainties and external disturbances. The simulation results demonstrate that our control strategy is effective in tracking high speed trajectories with less chattering, as compared to the conventional sliding mode control. The learning process of BLS is shown to enhance the performance of a new robust controller.

Lastly, we consider the potential field methodology to generate a desired trajectory in small and constrained environments. Also, Obstacle Collision Avoidance (OCA) is applied to obtain an inverse kinematic solution of a redundant robotic manipulator.

DEDICATION

To my mother, father, and sister

ACKNOWLEDGEMENTS

I would like to express my deepest gratitude to my advisors Dr. Reza Langari who gave me the necessary insight that I needed to get through this process. Also I want to thank my professor and fellow students at Texas A&M University. The learning environment that was there made me a better student and better prepared to pursue a doctorate. The completion of this dissertation would not have been possible without their support. The experiences that I had there will carry me for the rest of my life and I am forever indebted to my time there.

I also extend my gratitude to Dr. Richard Malak, Dr. Sivakumar Rathinam, Dr. Dylan Shell, and Dr. Dezhen Song for being on my committee. This dissertation has been improved by their comments and fruitful discussions.

Finally, especially thanks to my mother and father for their encouragement.

TABLE OF CONTENTS

Page

LIST OF FIGURES

FIGURE Page

LIST OF TABLES

CHAPTER I

INRODUCTION

With noted developments in technology, application of intelligent robot since 1990's has moved away from traditional automation industry towards medical, entertainment, and social safety, etc. [1, 2]. In this context, a variety of robots have been proposed for execution of tasks that require dexterous manipulation.

Among the developed robots, serial manipulators with fixed length links are broadly utilized in many fields [3]. These manipulators can in principle reach a large workspace, which easily leads to a variety of potential applications. For example, they may be used to deploy sensors and/or to provide assistance to victims of natural or man-made disasters. In this respect, reach-ability and maneuverability of the manipulator end-effector are particularly relevant and indeed can determine whether the manipulator can perform its intended function [4].

However, in constrained or complex environments, a robotic manipulator composed of a serial combination of discrete rigid links has a more restricted motion for performing the required tasks than it would in open spaces. Moreover, the closer the constrained link is relative to the base frame, the smaller the manipulator workspace. The activity area of these robotic manipulators is very limited, due to physical constraint conditions. To this end, this dissertation discusses an implementation of a design, control and motion planning for a novel extendable modular redundant robotic manipulator in

space constraints, which robots may encounter for completing required tasks in small and constraints environment.

Hyper-Redundant Robotic Manipulator

To overcome the previously explained shortcoming, many researchers have investigated a redundant robotic manipulator with surplus Degree Of Freedom (DOF) called the hyper-redundant robot. This serial manipulator can obtain the necessary configuration for the required task through additional DOFs.

Chirikjian and Burdick introduced the term hyper-redundant robots in [5, 6]. Yim [7] introduced modules to construct a hyper-redundant snake robot with modularity and the simplicity. Haith modified Yim's modules to give snake robots better performance in locomotion [8]. Takanashi, who developed a new two degrees-of-freedom joint for a more compact design, pioneered three-dimensional hyper-redundant robots [9]. Researchers at Jet Proportional Laboratory [10] modified Takanashi's design through using a universal joint in the interior of a robot. Some researchers have implemented to actuate joints with cables, but these require a large driving system that would not be realized with its internal degrees-of-freedom [11].

Redundancy Resolution

In a robotic manipulator, the manipulator's redundancy has been recognized as major characteristics in performing tasks that require dexterity. However, due to the redundancy, a redundant robotic manipulator needs for an inverse solution with

additional tasks for the desired configuration. Extra DOFs (beyond 6) can be used to fulfill user-defined additional tasks that are represented as kinematic functions.

There are two redundancy resolution approaches. The first approach is the generalized optimization method that converges to a local minimum of a cost function [12]. The other approach is an extended jacobian method that augments the jacobian of the main task [13] [14]. The cost functions selected to satisfy a performance criterion are usually as used: mathematical singularity avoidance [15], local torque minimization [16], flexible base vibration reduction [17], etc. Above all cost functions, joint limit avoidance [18] and obstacle collision avoidance [19] via the general projection method are developed by Liegeois and Kabit, respectively.

Manipulability Measurement

In order to design and analyze a serial redundant manipulator, the robotic manipulability is also core issue. It is the ability not only to change its end-effector in any position or orientation of its operational space at a given configuration but also to reach a certain set of positions in the defined workspace [20, 21, 22].

As a pioneer of the robotic manipulability analysis, Yoshikawa developed elements of the manipulability theory and defined the quantitative indexes for manipulability measure of a redundant manipulator [22, 23]. During last two decades, a number of manipulability measure methods have also been investigated by Gosselin and Angeles [24, 25, 26, 27]. Furthermore, the global task space manipulability for cooperating arm systems has been discussed by [28, 29].

Geometry Algorithms in Robotics

Traditionally, the Lagrangian approach can be useful for computing the equations of motion of open chain robotic systems. However, in case of a hyper-redundant robot, this approach is too burdensome to obtain the differential equations of motion. As the complexity of a robotic system increases, the needs for more elegant formulations of the equations of motion and for their computational efficiency become increasingly an issue of paramount importance.

Since 1980s, differential geometric methods have been applied to the study of robot kinematics and dynamics. It is the efficient geometric algorithm based on Lie groups and Lie algebra has been used for dynamic analysis [30, 31]. Brokett introduced the product of exponential (POE) equations for forward kinematics of serial chains with the theory of Lie groups [32].

In 1991, Samuel investigated the relationship between classical screw theory and Lie groups [33]. Bedrossian and Spong considered the Riemannian geometry to discuss a feedback linearization approach for a robotic manipulator [34]. Park and Ploen derived the equation of motion of open chains using Lie theory and Lagrange's equations [35, 36]. Also, they introduced the derivation of a geometric version of the recursive Newton-Euler in terms of generalized velocities and forces. Selig introduced both recursive Newton-Euler and Lagragian formulations of a robotic manipulator based on Lie theory [37]. Chen and Yang presented the equation of motion of a modular robot using a global matrix representation of recursive Newton-Euler algorithms [38].

Potential Filed Methodology

Moreover, due to the fact that the operational environment of a robot is the unknown terrain involving complex configuration spaces [39, 40], fast motion planning is the core issue. Given the limited information about the unknown terrain, robots need to be able to re-plan quickly, as their knowledge of the terrain changes [41].

Among famous methods of path planning, the potential field methodology provides a solution much faster than other heuristic algorithms [40]. This method generates the resulting vector field of potential field vectors as a guiding path for a robot to reach the goal. Generally, this method has been used for manipulator control [40, 41], obstacle collision avoidance [42], and local path planning [43, 44], etc. Suh and Shin [45] represented a path planning strategy to find an optimal path in two dimensions.

Sliding Mode Control Strategy

A robotic manipulator is a very strongly coupled nonlinear dynamic system with uncertainties [46, 47]. Because the uncertainty can undermine the desired performance, nonlinear robust control design should be required to fully exploit a robot's capabilities. Especially, due to needs for heavy mass and fast operation in the small and constrained environments, dynamic control of a robotic manipulator is able to provide better performance for completion of the required tasks in that situation, compared to kinematic control.

In 1980s, sliding mode control, derived from variable structure theory, was extensively used in robot control to ensure robustness against system uncertainties and

external disturbances [48, 49, 50]. While system states lie on the sliding mode, it provides the system the dynamics with invariance to modeling imprecision [51, 52, 53]. However, there are still unsolved drawbacks of a conventional sliding mode control. Chattering phenomena may excite high frequency dynamics, and knowledge of the bounded uncertainties is essential to obtain robustness and convergence [50]. To this end, many researchers have investigated diverse robust control strategies considering either chattering reduction or information acquisition of uncertainty bound [50, 54. 55].

However, it is very difficult to reduce the chattering phenomena while tracking high speed trajectories and to select the proper factor based on the bounds of uncertainties. So, the additional control techniques to deal with uncertainty and external disturbances are needed.

As one of famous methods, the on-line computed parameters achieve favorable system robustness regarding parameter uncertainties and external disturbances, instead of selection of the bound uncertainties [56]. Also, fuzzy sliding mode control is one of the approaches for solving the aforementioned problems [50, 55].

Brain Limbic System Control

The brain limbic system control strategy, initiated from computational modeling of the mammalian brain developed by Moren and Balkenius [57, 58], is based on an emotional learning and signal process mechanisms. They were not only to discover the effect of emotional learning behavior but also to develop a mathematical model,

associated on process of generating emotions. In Mowrer‘s two-process learning model, the emotional stimulus-response of humans is considered as the resulting cues [59].

In cognitive science, the brain limbic system control strategy (also referred to as BEBLIC; Brain Emotional Learning Based Intelligent Control) is applied to a wide range of research. In particular, as a pioneer of brain limbic system controller, Lucas et al. developed a controller based on Moren’s discovery and named Brain Emotional Learning Based Intelligent Controller [60]. A. R. Mehrabian and C. Lucas and et al utilized the brain limbic system controller to eliminate a tracking error in a flight control system [61]. The performance of the brain limbic system controller in autonomous robot and robotic manipulator are investigated in [62, 63].

Contributions and Outline of the Dissertation

The contribution of this study is to implement a Design, Control and Motion planning for an extendable modular redundant robotic manipulator in small and constraints environment.

Firstly, we design a novel robotic manipulator with appropriate levels of kinematic redundancy [64, 65, 66], adapted for constrained and complex environments. Then, we should generate the fast trajectory through applying the potential field and make a robot track it via a bio-inspired sliding mode control strategy. To this end, the following will be covered:

- To design a novel modular extendable robotic manipulator.
- To analyze the proposed robotic manipulator both kinematically and

dynamically.

- To optimize the structure of the robotic manipulator.
- To apply Obstacle Collision Avoidance (OCA) [66] both to prevent the robot from colliding with obstacles and to obtain an inverse kinematic solution.
- To apply a potential field method for generating a desired path in unknown terrain.
- To develop a bio-inspired sliding mode control strategy to track a reference path.

The remainder of this study is divided into seven chapters as follows. Designs of the proposed multiple DOFs link and the robotic manipulator are introduced in Chapter 2. Chapter 3 and Chapter 4 describe the kinematic and dynamic analyses of the proposed manipulator, respectively. With a choice of the obstacle collision avoidance as an additional task [66], the redundancy resolution is completed. A potential field method for the unknown terrain is applied as a navigation approach in Chapter 5. Furthermore, a novel robust sliding mode control with brain limbic system control strategy to track a reference path is explained in Chapter 6. In Chapter 7, all simulation results are explained. The conclusion and some mathematical calculations are placed in the last chapter and the Appendix.

CHAPTER II

A DESIGN OF THE PROPOSED ROBOTIC MANIPULATOR

The Design Objective

In constrained or complex environments, a robotic manipulator comprising discrete rigid links has a more restricted motion for performing the required tasks than it would in open spaces. Due to physical constraints conditions, the activity area of a robotic manipulator is very limited.

To this end, extendable modular robots with appropriate levels of kinematic redundancy have been proposed [3, 4]. In these studies, a large number of total degrees of freedom are aimed at enlarging the given manipulator's workspace and its manipulability, via added identical links. However, previously developed manipulators have not been adapted to complete their missions in small and constrained environments [3, 4]. First, in view of its geometry, there are natural disadvantages due to accumulated errors, with respect to its own volume and occupied floor space, compared to that of a few number of links [3]. Second, it is not guaranteed that the operational space is sufficient for the manipulator to operate with the increased links, in small or complex environments. It implies that a solution, by adding more links, is not always effective for constrained or small workspace environments. In other words, the traditional manipulator composed of single-DOF links cannot meet all its task requirements in small or constrained environments. This is especially true in a catastrophe, where a rescue robotic manipulator may encounter constraints from all directions.

In this study, the core design of the proposed robot is based on a modular reconfigurable robotic manipulator, to deal with the aforementioned issues. The proposed design, consisting of a serial chain of 3-DOFs links, manages to increase the robot's reach while also improving its manipulability, through replacing 1-DOF links with multi degree of freedom (3-DOF) links. This can increase the robot's total degree of freedom, eliminate singularities and improve dexterity without the addition of more rigid links. Particularly, the controllable length plays an essential part in having a relatively larger reachable workspace in constrained environments (in Figure 1).

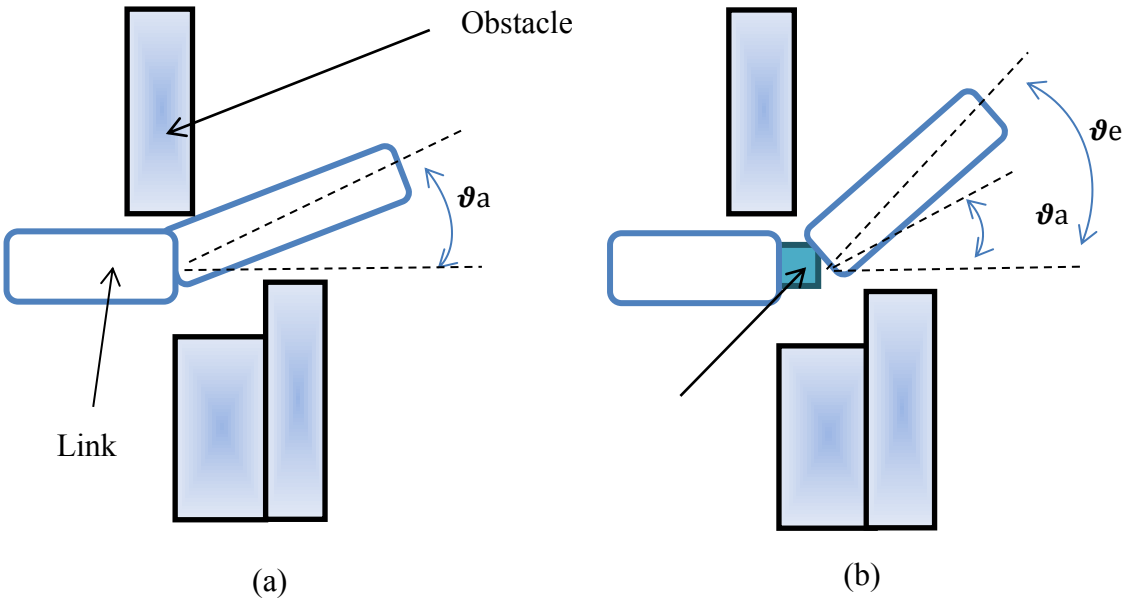

Figure 1. Two cases of manipulators (a) general link (θ_a) (b) an extensional link (θ_e)

3 DOFs Link Model

As can be seen in Figure 2, the proposed versatile 3-DOF link is composed of

three sub-systems. Two subsystems, the translation and the first rotation are embedded within the link. So, if these two subsystems are not operating, the mechanism of the link is the same as a rigid 1-DOF link. Each link is rectangular parallelepiped type.

The first subsystem, adjacent to the base frame, adjusts the link length between 180 mm and 210mm (i.e. by approximately 15%). The primary means of elongation through a ball screw mechanism and miniature linear guides. Two miniature linear guides prevent the bending of the link during translation.

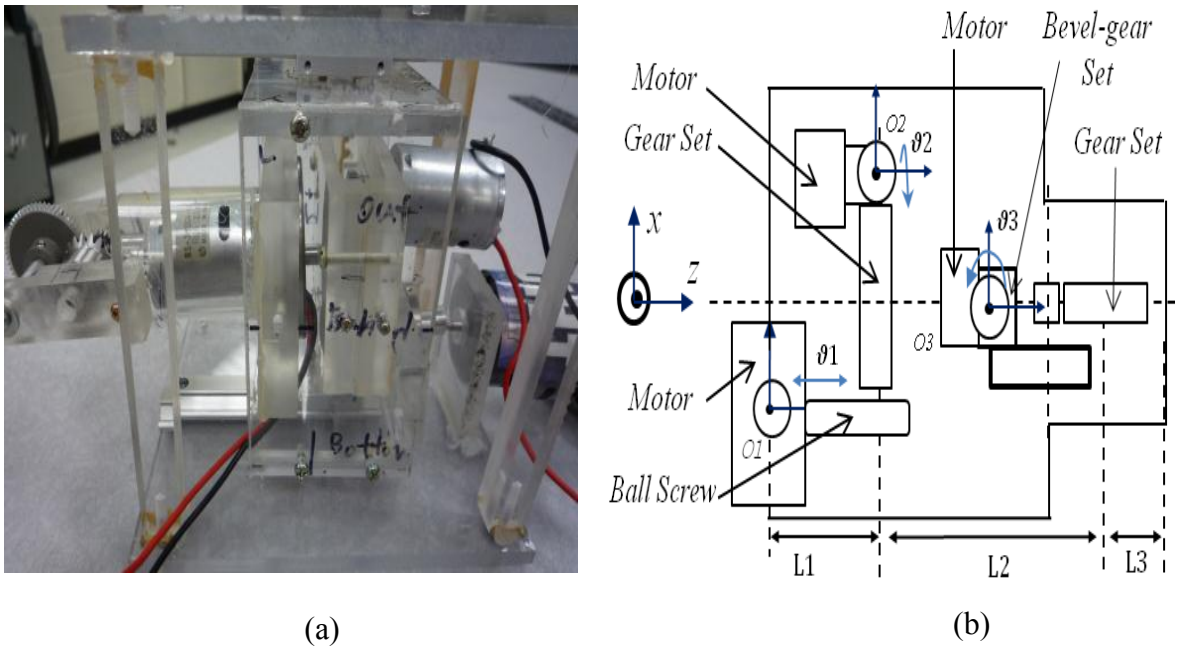

(a) (b)

Figure 2. The proposed link model (a) an overview (b) a descriptive schematic

The second motion subsystem supports the rotation of the link about its center axis. The challenging design of this subsystem is providing unconstrained rotational movement ($-180° \le \theta_2 \le 180°$). In addition, a spur-gear set is a significant tool for dealing

with the load resulting from multiple links. The centroid axes of the two subsystems are the same as the central axis of the link.

Figure 3. The third sub-system

The third motion subsystem has a constrained revolute joint ($-45° \leq \theta_2 \leq 45°$) that is located at the end of the link. As displayed in Figure 3, a bevel-gear set provides efficient transfer of motion between two adjacent links.

Design Optimization

Even though the proposed modular robotic manipulator has certain benefits such as simplicity or modularity, a cost of strength, range of motion, and low performance should be very considerable. Designing a robotic manipulator proves to be much more

difficult, due to the several conflicting design objectives that have to be addressed simultaneously [67].

So, we investigate the optimal design architecture of the proposed robotic manipulator concerning our design objectives. The total number of links decided by a design optimization can be useful distinction in practice [68].

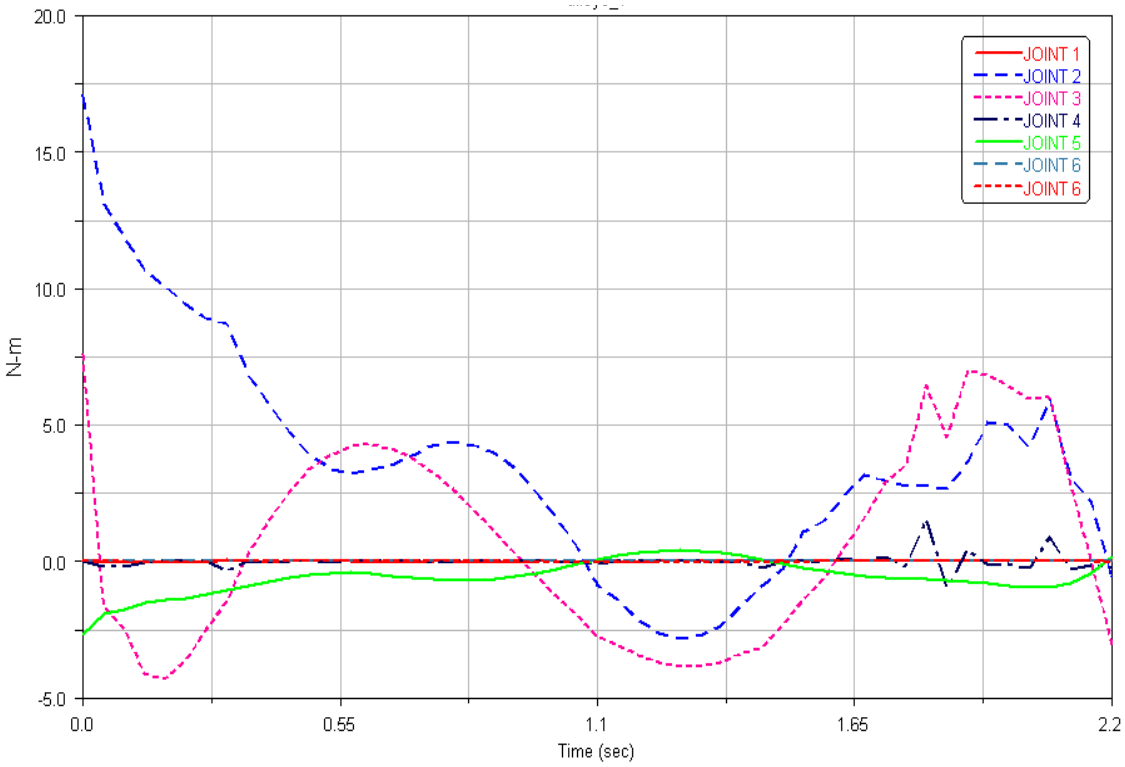

Figure 4. Torques at all joints in case study

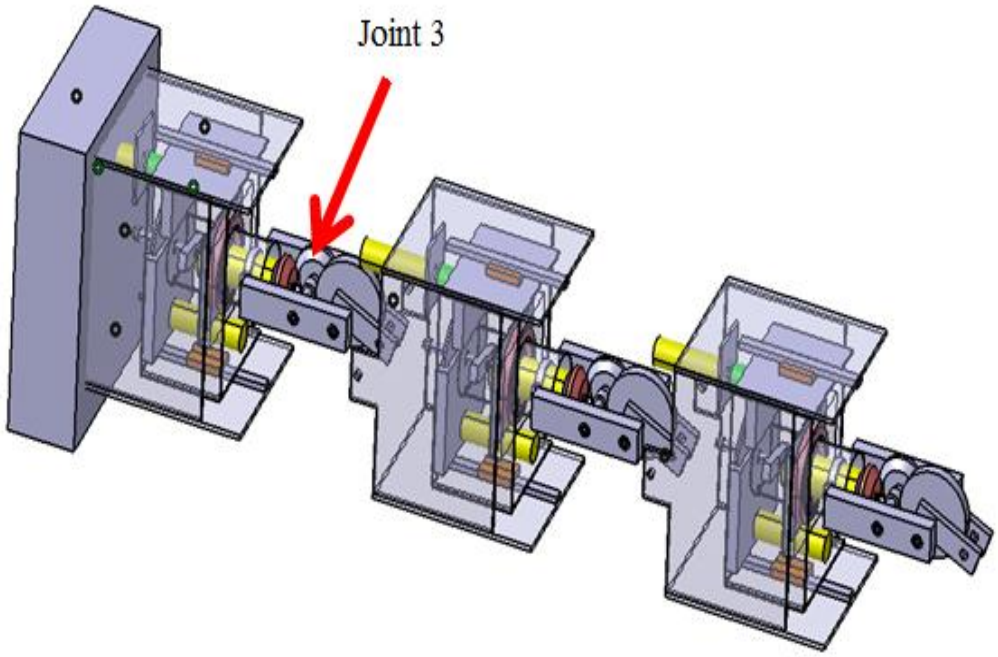

Figure 5. Joint 3 at a combination of three links

In this study, it is considered the number of links that produce an optimal solution give two objectives. The first objective is to produce a relatively large reachable workspace, which can help the proposed robotic system to operate with the large reachability. The second objective is to minimize the maximum static torque at the third joint (called Joint 3) in sequence from the base. Dynamic analysis (in Figure 4) shows that Joint 3 has to support with the maximum static torque compared to the others, given at the same range of motion (0 to 30 degree) of all joints simultaneously. However, because these two objectives are mutually conflicting, one cannot improve one without trading off against the other objectives.

Meanwhile, the volume of reachable workspace and the maximum static torque at Joint 3 are displayed in Equation (3). $W(i)$ and $\mathrm{T}(i)$ represent the volume of

reachable workspace and the maximum static torque (at the Joint 3) at a combination of *i* links (in Figure 5).

- 1 link and end-effector
  - Reachable Workspace: $W(1) = 0.5\pi L_3 L_3 L_0$
  - Max. torque: $T(1) = 0.125 L_3 M_3 g(\pi + \sqrt{2})$
- 2 links and end-effector
  - Reachable Workspace: $W(2) = (2.5\pi L_3 L_3 L_0 - 0.66\pi L_3 L_3 L_3 (2 - \sqrt{2}))$
  - Max. torque:$T(2) = 0.5(L_3 M_3 + (M1 + M2)(0.5L_1 + 0.5L_2 + L_3))g(\pi + \sqrt{2})$
- 3 link and end-effector (1)
  - Reachable Workspace: $W(3) = (9.5\pi L_3 L_3 L_0 - 3.5\pi L_3 L_3 L_3 (2 - \sqrt{2}))$
  - Max. torque:$T(3) = 0.5(1.5L_3 M_3 + (M_1 + M_2)(2L_1 + 2L_2 + 3L_3))g(\pi + \sqrt{2})$
- 4 link and end-effector
  - Reachable Workspace: $W(4) = (11.5\pi L_3 L_3 L_0 - 19.5\pi L_3 L_3 L_3 (2 - \sqrt{2})))$
  - Max. torque: $T(4) = 0.5(2L_3 M_3 + (M_1 + M_2)(4.5L_1 + 4.5L_2 + 6L_3))g(\pi + \sqrt{2})$

As displayed in Figure 6, set of alternatives in our study are mutually non-dominating. This non-dominated set should be considered to solve the multi-objective optimization problem.

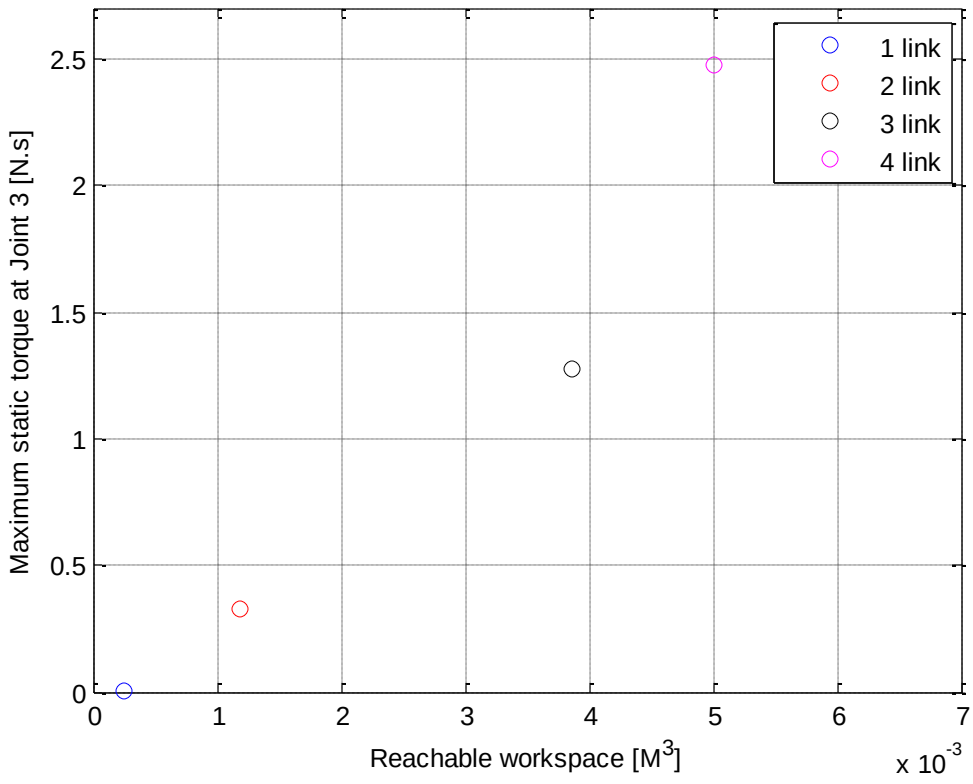

Figure 6. Reachable workspace and maximum static torque in decision objective space

The general multi-objective optimization problem is described as [69, 70]:

$$\begin{aligned} &\min_{x} \quad F(x) = [(F_1(x), F_2(x), \cdots, F_k(x)]^T \in E^n, \\ &\textit{subject to} \quad g_j(x) \le 0, j = 1, \cdots, m, \\ &\qquad\qquad h_l(x) = 0, l = 1, \cdots, p, \end{aligned} \tag{2}$$

where k, m, and p are the number of objective functions, inequality constraints, and equality constraints respectively. $x \in E^n$ is a vector of decision variables where n is the number of independent variables x_i. F_i is called the cost functions.

With application of the weighted sum aggregation function, a multi-objectives problem in our study over a subset of feasible decisions (referred as the decision space [68, 71]) is mathematically addressed as follow,

$$\begin{aligned} X_i &= Arg\max_i[\alpha_1 \cdot W(i) + \alpha_2 \cdot T(i)], \\ &subject\ to\ i = 1, \cdots, 4, \\ &g_j(i) \le 0,\ j = 1, \cdots, m, \\ &h_k(i) = 0, k = 1, \cdots, p, \end{aligned} \tag{3}$$

where α_1 and α_2 are the weighted values between 0 and 1. g_j and h_k are the inequality and equality constraints, respectively.

In decision objective space [68, 71], Equation (3) can be rewritten as

$$\begin{aligned} X_i &= Arg\max_i[AU(W(i), T(i))], \\ &subject\ to\ i = 1, \cdots, 4, \\ &h_k(i) = 0, k = 1, \cdots, p, \end{aligned} \tag{4}$$

where $AU(W(i), T(i))$ represents the sum aggregate utility function regarding the aforementioned objectives. As displayed in Figure 7, the utility functions regarding two objectives can be defined by considering the physical significance of the relevant quantities.

Through the multi-linear utility elicitation [71, 72], a utility function in this study can be expressed as

$$AU(i) = K_1 \cdot U_1(W(i)) + K_2 \cdot U_2(T(i)), \tag{5}$$

where $K_1 (= 0.65)$ and $K_2 (= 0.35)$ are selectable constants.

Figure 8 represents the preference of the sum aggregate utility regarding our objectives. From the Figure 8, the robotic architecture comprising two connected links and an end-effector is said to have the highest preference of utility [73, 74].

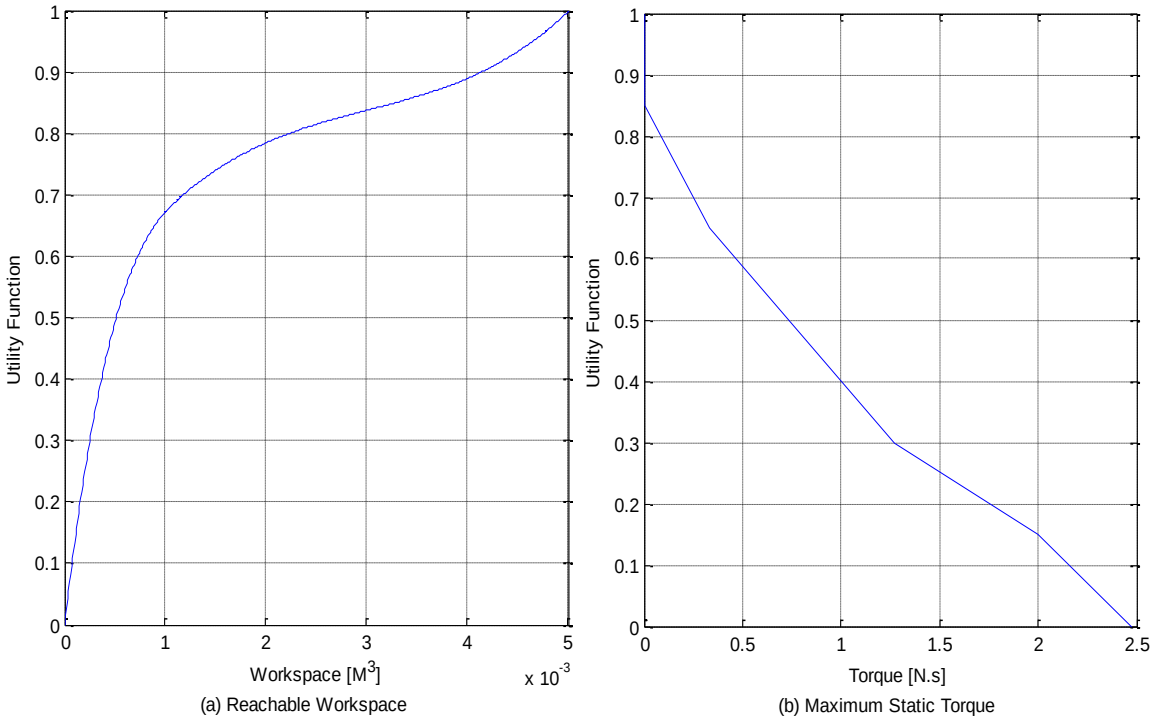

Figure 7. Utility functions for reachable workspace and maximum static torque

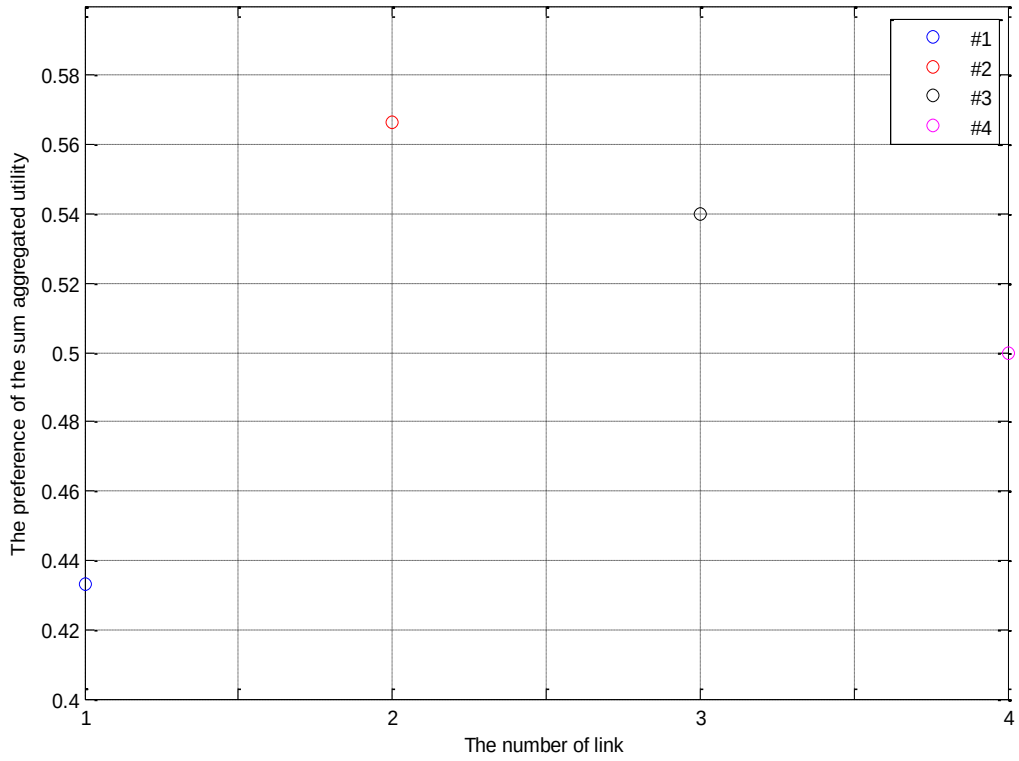

Figure 8. The preference of the sum aggregate utility

Robotic Manipulator

Figure 9.a describes the overall structure of the proposed manipulator, which is a serial-chain with two identical 3-DOFs links (discussed in the precious chapters) in addition to an end-effector. Coordinate frames of the proposed manipulator are shown in Figure 9.b.

The proposed design, the Expandable Modular Self-Reconfigurable Robot, has the properties of versatility for given tasks, robustness (replacement by an identical module) [75, 76]. It should be noted that our robotic manipulator can be extended to more than two identical links although the present study focuses on this limited version.

Furthermore, this fact provides that both the compactness and the maneuverability properties of our proposed design make it suitable for constructing the hyper-redundant robots through reconfiguration process.

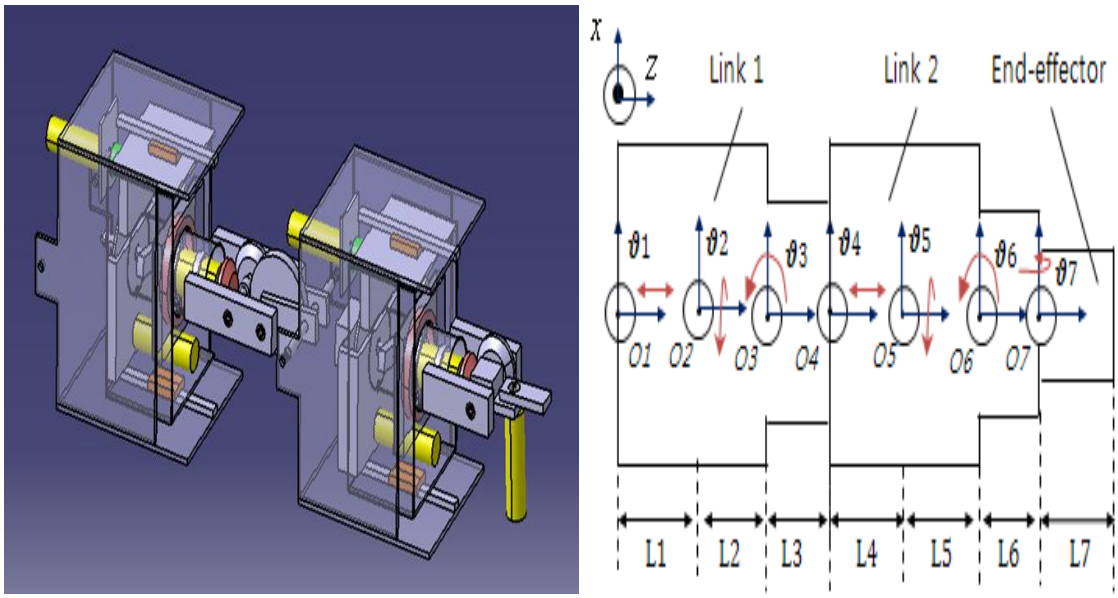

(a) (b)

Figure 9. The designed serial manipulator (a) overview (b) coordinate frames

CHAPTER III

KINEMATICS

The kinematics of a manipulator describes the relationship between the individual joint variables of the robot and the posture of the end-effector. In this chapter, kinematics is represented by the product of exponentials using concepts from the theory of Lie groups [27, 77, 78, 79].

Forward Kinematics

Given a task, the forward kinematics is concerned with the configuration of the end-effector by the motion of the individual joints. The motion is associated with rotation and translation along the axis of twist. The Special Euclidean group, $SE(3) = R^3 \times SO(3)$, is the semi-direct product of R^3 with the Special Orthogonal group, $SO(3) = \left\{ R \in R^3 \times R^3 : RR^T = I, det(R) = +1 \right\}$.

The forward kinematics map of a manipulator, $g_{st} : Q \to SE(3)$, is given by [27]:

$$g_{st}(\theta) = e^{\hat{\xi}_1} e^{\hat{\xi}_2} \cdots e^{\hat{\xi}_{n-1}} e^{\hat{\xi}_n} g_{st}(0), \tag{7}$$

where $i = 1, \cdots, n$ and $\theta_i \in Q$. ξ_i and θ_i are the twist coordinates and the amount of motion associated with the ith joint, respectively.

Let $\xi = [a_1 \; a_2 \; a_3]^T \in R^3$ and $\hat{\xi} = [0 \; -a_3 \; a_2 \; ; \; a_3 \; 0 \; -a_1 \; ; \; -a_2 \; a_1 \; 0]$ be a unit vector and its matrix which state the direction of twist axis and its Special Orthogonal group.

For the revolute joint,

$$\xi_i = \begin{bmatrix} -w_i \times q_i \\ w_i \end{bmatrix}, \tag{8}$$

where $w_i \in R^3$ and $q_i \in R^3$ are a unit vector pointing in the direction of the axis ith. For a prismatic joint,

$$\xi_i = \begin{bmatrix} v_i \\ 0 \end{bmatrix}, \tag{9}$$

where $v_i \in R^3$ is a unit vector in the direction of the translation .

For the two translational joints along the z direction:

$$\begin{aligned} \xi_1 &= \begin{bmatrix} 0 & 0 & 1 & 0 & 0 & 0 \end{bmatrix}^T, \\ \xi_4 &= \begin{bmatrix} 0 & 0 & 1 & 0 & 0 & 0 \end{bmatrix}^T. \end{aligned} \tag{10}$$

The twists for the revolute joints are as follows:

$$\begin{aligned} \xi_2 &= \begin{bmatrix} 0 & 0 & 0 & 0 & 0 & 1 \end{bmatrix}^T, \\ \xi_3 &= \begin{bmatrix} l_1 + l_2 & 0 & 0 & 0 & 1 & 0 \end{bmatrix}^T, \\ \xi_5 &= \begin{bmatrix} 0 & 0 & 0 & 0 & 0 & 1 \end{bmatrix}^T, \\ \xi_6 &= \begin{bmatrix} l_1 + l_2 + l_4 + l_5 & 0 & 0 & 0 & 1 & 0 \end{bmatrix}^T, \\ \xi_7 &= \begin{bmatrix} 0 & 0 & L & 1 & 0 & 0 \end{bmatrix}^T. \end{aligned} \tag{11}$$

From Figure 9.b, $g_{st}(0)$ represents the rigid body transformation between the base frame (attached to the first link) and the end-effector frame for $\theta_i = 0, i = 1, \cdots, 7.$, is given by:

$$g_{st}(\mathrm{O}) = \begin{bmatrix} & \mathbf{O} \\ \boldsymbol{I} & \mathbf{O} \\ & \boldsymbol{L} \\ \mathbf{O} & 1 \end{bmatrix} \qquad \text{where } L = l_1 + l_2 + \cdots + l_7 \tag{12}$$

Consequently, the kinematic map of the proposed manipulator is addressed in:

$$g_{st}(\theta) = e^{\hat{\xi}_1} e^{\hat{\xi}_2} \cdots e^{\hat{\xi}_6} e^{\hat{\xi}_7} g_{st}(0) = \begin{bmatrix} T_{11} & T_{12} & T_{13} & T_{14} \\ T_{21} & T_{22} & T_{23} & T_{24} \\ T_{31} & T_{32} & T_{33} & T_{34} \\ 0 & 0 & 0 & 1 \end{bmatrix}, \tag{13}$$

where $c_i = \cos\theta_i, s_i = \sin\theta_i$

$$T_{11} = c_6(c_2c_3c_5 - s_2s_5) - c_2s_3s_6, T_{12} = -c_7(c_2c_3s_5 + s_2c_5) + (c_2s_3c_6 + s_6(c_2c_3c_5 - s_2s_5))s_7,$$

$$T_{13} = s_7(c_2c_3s_5 + s_2c_5) + (c_2s_3c_6 + s_6(c_2c_3c_5 - s_2s_5))c_7,$$

$$T_{14} = (l_3 + l_4 + l_5 + q_4 + l_6c_6)c_2s_3 + (c_2c_3c_5 - s_2s_5)(l_6s_6 + l_7s_6c_7) + l_7(c_2s_3c_6c_7 + s_2c_5s_7 + c_2c_3s_5s_7),$$

$$T_{21} = c_6(s_2c_3c_5 + c_2s_5) - s_2s_3s_6,$$

$$T_{22} = c_7(-s_2c_3s_5 + c_2c_5) + (s_2s_3c_6 + s_6(s_2c_3c_5 + c_2s_5))s_7,$$

$$T_{23} = s_7(s_2c_3s_5 - c_2c_5) + (s_2s_3c_6 + s_6(s_2c_3c_5 + c_2s_5))c_7,$$

$$T_{24} = (l_3 + l_4 + l_5 + q_4 + l_6c_6)s_2s_3 + (s_2c_3c_5 + c_2s_5)(l_6s_6 + l_7s_6c_7) + l_7(s_2s_3c_6c_7 - c_2c_5s_7 + s_2c_3s_5s_7),$$

$$T_{31} = -c_3s_6 - s_3c_5c_6, T_{32} = s_3s_5c_7 + (c_3s_5 - s_3c_5s_6)s_7, T_{33} = -s_3s_5s_7 + (c_3c_6 - s_3c_5s_6)c_7,$$

$$T_{34} = l_1 + l_2 + q_1 + (l_3 + l_4 + l_5 + q_4 + l_6c_6)c_3 + (l_6 - l_7c_7)s_3c_5s_6 + l_7(c_3c_6c_7 - s_3s_5s_7)$$

Jacobian Matrix

Differential kinematics describes the relationship between the joint velocities and the linear and angular velocity of the end-effector. This mapping, called the Jacobian, is

useful for analyzing singularities, redundancy or manipulability and determining the inverse kinematic algorithm [37, 80]. Traditionally, it is obtained by differentiating the forward kinematics map. However, if we define the forward kinematics as $g_{st}: Q \to SE(3), \theta \in Q$, it is not easy to obtain the Jacobian, due to the fact that g_{st} is a matrix-valued function [80]. The instantaneous spatial velocity of the end-effector is given by [27]:

$$V = \dot{g}_{st}(\theta)\dot{g}_{st}^{-1}(\theta) \tag{14}$$

After applying the chain-rule, the relationship between the velocity of the individual joints and the end-effector is linear as in Equation (15). The resulting velocity of the manipulator is as follows [27]**:**

$$V = \sum_{i=1}^{n}(\frac{\partial g}{\partial \theta_i}\dot{\theta}_i)g^{-1}(\theta) = \sum_{i=1}^{n}(\frac{\partial g}{\partial \theta_i}g^{-1}(\theta))\dot{\theta}_i = J(\theta)\dot{\theta}, \tag{15}$$

$$\text{where } J(\theta) = [\xi_1' \ \cdots \ \xi_n'], \xi_i' = Ad_{\left(e^{\xi_1\theta_1}\cdots e^{\xi_{i-1}\theta_{i-1}}\right)}\xi_i.$$

$$Ad_{(T)} = \begin{bmatrix} R(t) & \hat{p}R(t) \\ 0 & R(t) \end{bmatrix}$$

$Ad_{(T)}$ is the adjoint representation of $T(t) = \begin{bmatrix} R(t) & p(t) \\ 0 & 1 \end{bmatrix}$ with $(p(t), R(t)) \in SE(3)$.

$$J(\theta) = \begin{bmatrix} J_{11} & \cdots & J_{17} \\ \vdots & \ddots & \vdots \\ J_{61} & \cdots & J_{67} \end{bmatrix}, \tag{16}$$

where $c_i = \cos\theta_i, s_i = \sin\theta_i$

$$J_{11} = 0,\ J_{12} = 0,\ J_{13} = -c_2(l_1 + l_2 + \theta_1),\ J_{14} = c_2 s_3,\ J_{15} = -s_2 s_3(l_1 + l_2 + \theta_1),$$
$$J_{16} = (l_1 + l_2 + \theta_1)(s_2 c_3 c_5 - c_2 c_5) + (l_3 + l_4 + l_5 + \theta_4)(s_2 c_5 - c_2 c_3 c_5),$$
$$J_{17} = -(l_1 + l_2 + \theta_1)(s_2 c_3 c_5 c_6 + c_2 c_5 c_6 - s_2 s_3 s_6) + ((l_3 + l_4 + l_5 + \theta_4)c_6 + l_6)(-c_2 c_5 + s_2 c_3 c_5),$$
$$J_{21} = 0,\ J_{22} = 0,\ J_{23} = -s_2(l_1 + l_2 + \theta_1),\ J_{24} = s_2 s_3,\ J_{25} = c_2 s_3(l_1 + l_2 + \theta_1),$$
$$J_{26} = -(l_1 + l_2 + \theta_1)(s_2 c_5 + c_2 c_3 c_5) - (l_3 + l_4 + l_5 + \theta_4)(c_2 s_5 + s_2 c_3 c_5),$$
$$J_{27} = -(l_1 + l_2 + \theta_1)(c_2 c_3 c_5 c_6 - s_2 c_5 c_6 - c_2 s_3 s_6) + ((l_3 + l_4 + l_5 + \theta_4)c_6 + l_6)(-c_2 c_5 + s_2 c_3 c_5),$$
$$J_{31} = 1,\ J_{32} = 0,\ J_{33} = 0,\ J_{34} = c_3,\ J_{35} = 0,\ J_{36} = s_3 c_5(l_3 + l_4 + l_5 + \theta_4),$$
$$J_{37} = s_3 s_5((l_3 + l_4 + l_5 + \theta_4)c_6 + l_6),\ J_{41} = 0,\ J_{42} = 0,\ J_{43} = 0,\ J_{44} = 0,\ J_{45} = c_2 s_3,$$
$$J_{46} = s_2 c_5 + c_2 c_3 c_5,\ J_{47} = c_2 c_3 c_5 c_6 - s_2 s_5 c_6 - c_2 s_3 s_6, J_{51} = 0,\ J_{52} = 0,\ J_{53} = 0,$$
$$J_{54} = 0,\ J_{55} = s_2 s_3,\ J_{56} = -c_2 c_5 + s_2 c_3 c_5,\ J_{57} = s_2 c_3 c_5 c_6 + c_2 s_5 c_6 - s_2 s_3 s_6,$$
$$J_{61} = 0,\ J_{62} = 0,\ J_{63} = 0,\ J_{64} = 0,\ J_{65} = c_3,\ J_{66} = s_3 s_5,\ J_{67} = -c_3 s_6 - s_3 c_5 c_6$$

Redundancy Resolution (Obstacle Collision Avoidance)

The typical inverse kinematic solution is a matter of determining the joint variables, corresponding to a desired end-effector state [24, 27, 81]. Due to the redundancy of a proposed manipulator, multiple inverse solutions for the desired configuration are found [82]. To resolve mentioned difficulty in this study, the extended jacobian method with singular value decomposition is used in this paper [83].

Given a forward kinematic map, the desired configuration can be obtained as follows.

$$Y = \begin{bmatrix} X \\ Z \end{bmatrix} \tag{17}$$

where X and Z are the main task vector ($m \times 1$) and additional task vector($k \times 1$).

Therefore, augmented differential kinematics can be described as

$$\dot{Y} = \begin{bmatrix} \dot{X} \\ \dot{Z} \end{bmatrix} = \begin{bmatrix} J_x \\ J_z \end{bmatrix} \dot{\theta}$$

(18)

where $\dot{\theta}$ is the differential of the joint space vector ($n \times 1$). With this choice of the arbitrary vector Z in Equation (17), the optimal approach to the null space of the Jacobian can be obtained [83, 84]. Furthermore, a singularity robust and task prioritized formulation using the weighted damped least-squares method is utilized in this study [84, 85]. It can be represented as

$$\dot{\theta} = \left[J_x^T W_x J_x + J_z^T W_z J_z + W_v \right]^{-1} \left[J_x^T W_x \dot{X}^d + J_z^T W_z \dot{Z}^d \right] \tag{19}$$

$$subjec\ to \quad \min \left[\dot{E}_x^T W_x \dot{E}_x + \dot{E}_z^T W_z \dot{E}_z + \dot{\theta}^T W_v \dot{\theta} \right]$$

where $W_x(m \times m), W_z(k \times k), W_v(n \times n)$ are positive-definite weighting matrices about main, additional, and singular robust task: X^d, Z^d are desired trajectories of *X* and *Z*, respectively. $\dot{E}_x = \dot{X} - \dot{X}_d$ and $\dot{E}_z = \dot{Z} - \dot{Z}_d$ are the residual velocity errors of the main and additional tasks respectively.

In this study, Obstacle Collision Avoidance (OCA) [86] is selected as a performance criterion, as displayed in Figure 10. The additional kinematic function on the ith link is designated as the distance from each obstacle. The effective function of OCA is considered as Equation (20)

$$Z_i = g_i(\theta, t) = R_o - d_{c_i} \tag{20}$$

where t, R_o, d_{c_i} are time, Surface of Influence (SOI) and the critical distance, respectively.

The derivative of the additional kinematic function is

$$\dot{Z}_i = \frac{\partial g_i}{\partial \theta}\dot{\theta} + \frac{\partial g_i}{\partial t} = -u_i^T \left(\frac{\partial X_{c_i}}{\partial \theta}\dot{\theta} + \dot{X}_o \right) \tag{21}$$

For a static object, the Jacobian of the active constraints is

$$J_{c_i} = -u_i^T \frac{\partial X_{c_i}}{\partial \theta}\dot{\theta} \tag{22}$$

Furthermore, an inequality constraint subject to the defined buffer region (called surface of influence region) is applied [86]. Its conditions are displayed in Table 1.

Table 1. Inequality constraints conditions

Condition	Constraint	Weighting matrix
$d_{c_i} > SOI$:	All inactive constraints	$W_x = I, W_z = W_v = 0$
$d_{c_i} \le SOI$:	one or more active constraints	$W_x \neq 0, W_z \neq 0, W_v \neq 0.$

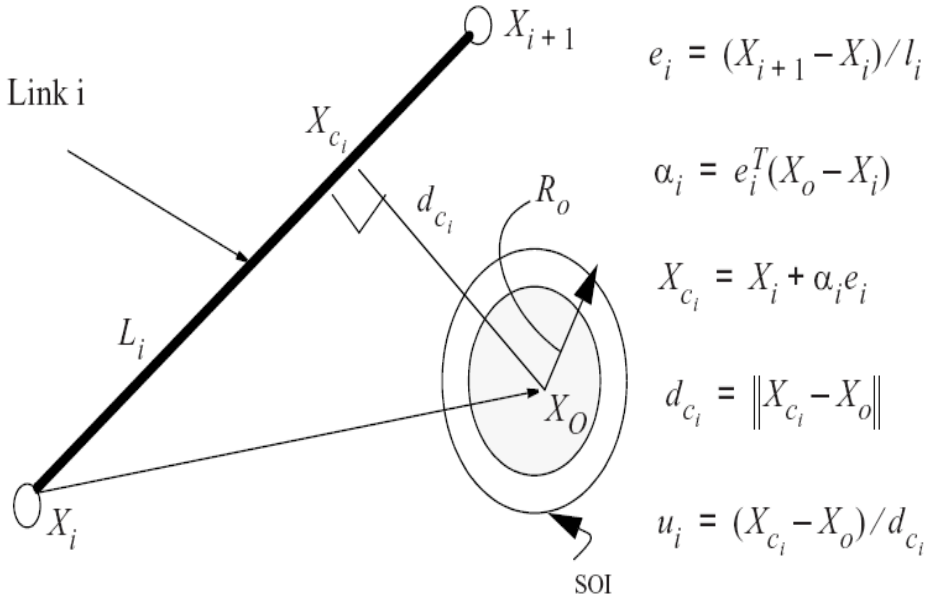

Figure 10. The critical distance calculation [66]

Singularity

Kinematic singularities are of great importance in the design and control of a robotic manipulator. The singular configurations would mean the feasibility of the reconfiguration into a nonsingular posture [20].

Kinematic singularities of a robotic manipulator occur when the Jacobian matrix has a rank deficit [24]. Considering that our manipulator is redundant, a kinematic configuration is singular if and only if the following conditions hold [87],

$$rank(J \cdot J^T) = rank(J) < 6. \tag{23}$$

With the above considerations, we enumerate all the analytical conditions of the kinematic singularities for the proposed 7-DOFs redundant manipulator, as in Table 2:

Table 2. Kinematic singularity

No.	Singularity Condition			
1	$\theta_2=(2n\pm1)\pi/4$	$\theta_3=2n\pi$		$\theta_6=(2n\pm1)\pi/2$
2	$\theta_2=(2n\pm1)\pi/4$	$\theta_3=2n\pi$	$\theta_5=(4n-1)\pi/4$	
3	$\theta_2=(2n\pm1)\pi/4$	$\theta_3=2n\pi$	$\theta_5\neq(2n-1)\pi/2$	$\theta_6=L_6/(3B)$
4	$\theta_2=(2n\pm1)\pi/4$	$\theta_3=(2n-1)\pi$	$\theta_5=(2n-1)\pi$	$\theta_6=(2n-1)\pi$
5	$\theta_2=(2n\pm1)\pi/4$	$\theta_3=(2n-1)\pi$	$\theta_5=\tan^{-1}[B/(A+B)]$	$\theta_6=\cos^{-1}[-2BL_6/(AA+AB+2BB)]$
6	$\theta_2\neq n\pi/2$	$\theta_3=(2n-1)\pi$	$\theta_5=(2n-1)\pi$	
7	$\theta_2=(2n-1)\pi$	$\theta_3=2n\pi$	$\theta_5=(2n-1)\pi$	$\theta_6=\cos^{-1}[L_6/(c3A-c3-B)]$
8	$\theta_2=(2n-1)\pi$	$\theta_3=(2n-1)\pi$		
9	$\theta_2=n\pi$	$\theta_3=(2n-1)\pi$	$\theta_5=(2n-1)\pi$	
10	$\theta_2=n\pi$	$\theta_3\neq n\pi/2$	$\theta_5=(2n-1)\pi$	$\theta_6=(2n-1)\pi$
11	$\theta_2=2n\pi$	$\theta_3=(2n+1)\pi/2$	$\theta_5\neq n\pi/2$	$\theta_6\neq n\pi$
12	$\theta_2=2n\pi$	$\theta_3=(2n-1)\pi/2$	$\theta_5=n\pi$	$\theta_6\neq n\pi$

where $A=L_1+L_2+L_3+\theta_1$, $B=L_4+L_5+L_6+\theta_4$

Manipulability

The manipulability measure in robotics is classified into two concepts. The first concept is the ability to reach a certain set of positions in the defined workspace. The other is the ability to change its end-effector in any position or orientation of its operational space at a given configuration. The latter, called local property around a

given configuration [27, 37], is utilized to characterize the manipulability of the proposed manipulator.

The Manipulability Ellipsoid, a geometric interpretation of the scaled eigenvectors, is used to measure the ability of an end-effector to move freely in all directions of the operational space [22, 23]. It describes the maximum available performance of a manipulator in positioning and orienting an end-effector [29]. Based on singular value analysis, it is defined as a set of end-effector velocities in response to individual joints velocities, belonging to a unit sphere [88, 89]. With the maximum values of individual joints ($|\dot{\theta}_i| \le \dot{\theta}_{i,\max}, i = 1, 2, \cdots, i$), the normalized joint velocities are represented as,

$$\tilde{\dot{\theta}} \le R^{-1}\dot{\theta}, \tag{24}$$

where $R = diag[\ \dot{\theta}_{1,\max}\ \cdots\ \dot{\theta}_{7,\max}\ ]$,

$$\tilde{\dot{\theta}} = diag[\ \frac{\dot{\theta}_1}{\dot{\theta}_{1,\max}}\ \cdots\ \frac{\dot{\theta}_7}{\dot{\theta}_{7,\max}}\ ]^T$$

The new scaled Jacobian matrix is

$$V = J\dot{\theta} = JR\tilde{\dot{\theta}} = \tilde{J}\tilde{\dot{\theta}} \tag{25}$$

With Equation (24) and (25), the Manipulability Ellipsoid can be rewritten as follows,

$$\tilde{\dot{\theta}} = \tilde{J}^{+}\tilde{V}, \ \text{since} \left\| \tilde{\dot{\theta}}_i \right\| \le 1 \tag{26}$$

$$V^T (\tilde{J}^+)^T \tilde{J}^+ V \leq 1 \tag{27}$$

We can derive the manipulability ellipsoid equations for linear velocity and angular velocity of our manipulator based on a given condition. The approximate resultant ellipsoids in translational velocity space and rotational velocity space are described as follows,

$$8.00e^{-5} \times X^2 + 1.99e^{-5} \times Y^2 + 0.001 \times Z^2 \leq 1 \tag{28}$$

$$1.0822 \times \theta_X{}^2 + 0.5564 \times \theta_Y{}^2 + 0.6506 \times \theta_Z{}^2 \leq 1 \tag{29}$$

where $[\dot{\theta}_{1,\max} \cdots \dot{\theta}_{8,\max}] = [\pi/4\ \pi/4\ \pi/4\ \pi/4\ \pi/4\ \pi/4\ \pi/4\ \pi/4]$ and $[\theta_{1,\max} \cdots \theta_{7,\max}] = [\pi/8\ \pi/8\ \pi/6\ \pi/8\ \pi/8\ \pi/6\ \pi/8]$.

As a pioneer of the manipulability, Yoshikawa has defined the quantitative indices for manipulability measure of redundant manipulators [85, 86]. The condition number, denoted by, $\tilde{C}_e$, is defined as the ratio of the maximum and minimum singular values of the Jacobian matrix [83]. His criterion reflects the distance of a given configuration from singularity. It is expressed as,

$$\tilde{C}_e = \frac{\tilde{\sigma}_1}{\tilde{\sigma}_6} = 1.5 \times 10^{-5} \tag{30}$$

where $\tilde{\sigma}_i = 1, \cdots, 6$ are singular values of the normalized Jacobian matrix in descending order. This qualitative value is involved in not only the shape of the ellipsoids but also the movement ability of the manipulator in any arbitrary direction. It is equal to the ratio between the minor axes and major axes of the ellipsoid [83].

CHAPTER IV

DYNAMICS

Traditionally, the Lagrangian approach is considered as the powerful method for computing the equation of motion of open chain robotic systems explicitly. However, deriving the differential equation of motion of a hyper-redundant robot via the Lagrangian way is too burdensome. As the complexity of a robotic system increases, the needs for more elegant and efficient formulations of the equation of motion become increasingly an issue of paramount importance.

The equation of motion is generated via Lagrange's equations as follows [80]:

$$\frac{d}{dt}\left(\frac{\partial L}{\partial \dot{q}_k}\right) - \frac{\partial L}{\partial q_k} = Q_k,\ k = 1, 2, \cdots, n, \tag{31}$$

where $L(q, \dot{q}) = T(q, \dot{q}) - V(q)$ is a scalar function. Here, $T(q, \dot{q})$ and $V(q)$ denote the total kinetic energy of the system and the total potential energy. q_i and Q are joint angle at each joint and a vector representing the generalized forces acting on the system.

The kinetic energy of a robotic system can be described:

$$T = \frac{1}{2}\sum_{i=1}^{n}\sum_{j=1}^{n} M_{ij}(q)\dot{q}_i\dot{q}_j \tag{32}$$

where $M_{ij} \in R^{n\times n}$ is a symmetric positive definite matrix. Upon substitution of Equation (32) into Equation (31), the Equation (31) can be rewritten as the following standard form,

$$M(q)\ddot{q} + C(q, \dot{q})\dot{q} + \phi(q) = \tau \tag{33}$$

where $M(q)$, $C(q, \dot{q})$, $\phi(q)$, and τ denote the mass matrix, the coriolis/centrifugal matrix, the gravity terms, and the applied torques.

In this Chapter, we primary present the dynamic analysis of the proposed robotic manipulator using techniques and notation from the theory of Lie groups and Lie algebras [35, 36]. This approach shows that the differential equations of motion which can be expressed in an explicit fashion that has computational efficiency [35, 36]. A simple global matrix form expressed entirely in terms of a coordinate invariant formulation is originally given in [36, 90].

A recursive formulation is a two-step iteration process [90]. Firstly, the forward iteration propagates the generalized velocities and accelerations of each link, expressed in local reference frames attached at the joint of each link, from the base toward the tip. Conversely, the backward iteration generates the generalized forces and torque, propagated backward from tip to base, in local reference frames expressed in the forward iteration.

Note that the following definitions are utilized in the corresponding link frame coordinates. Let $V_i \in R^{6\times1}$ and $\tau_i \in R^{6\times1}$ be the generalized velocity and the applied torque at link i. The $F_i \in R^{6\times1}$ be total generalized force transmitted from link i-1 to link i through joint i. Also, let $f_{i-1,i} = M_i e^{S_i q_i}$ denote the position and orientation of the link i frame relative to the link i-1 frame with $M_i \in SE(3)$ and $S_i = (\omega_i, 0) \in se(3)$ (here ω_i is a unit vector along the axis of rotation of joint i). Let J_i is defined as

$$J_i = \begin{bmatrix} I_i - \mathrm{m}_i[r_i]^2 & \mathrm{m}_i[r_i] \\ -\mathrm{m}_i[r_i] & \mathrm{m}_i I_{3\times 3} \end{bmatrix} \tag{34}$$

where M_i is the mass of link i, r_i is the vector in link i coordinates from the origin of the link i frame to the center of mass of link i, I_i is the inertia tensor of link i about the center of mass, and $I_3\times_3$ denotes the 3×3 identity matrix. Note that the Lie bracket and other mathematical expressions are explained in Appendix.

The recursive representation can be described as follows.

Initialization : Given :

$$V_0, \dot{V}_0, F_{n+1}. \tag{35}$$

Forward for i = 1 to n

recursive :

$$\begin{aligned} f_{i-1,i} &= M_i e^{S_i q_i}, \\ V_i &= Ad_{f_{i-1,i}^{-1}}(V_{i-1}) + S_i \dot{q}_i, \\ \dot{V}_i &= S_i \ddot{q}_i + Ad_{f_{i-1,i}^{-1}}(\dot{V}_{i-1}) - ad_{S_i \dot{q}_i} Ad_{f_{i-1,i}^{-1}}(V_{i-1}). \end{aligned} \tag{36}$$

Backward for i = n to 1

recursive:

$$\begin{aligned} F_i &= Ad^*_{f_{i+1,i}^{-1}}(F_{i+1}) + J_i \dot{V}_i - ad^*_{V_i}(J_i V_i), \\ \tau_i &= S_i^T F. \end{aligned} \tag{37}$$

Here, $V_0, \dot{V}_0$ denote the generalized velocity and acceleration of the base respectively, and F_{n+1} denotes the generalized force acting at the tip. Generally,

$V = 0, \dot{V} = 0, F_{n+1} = 0$ are assumed where $g \in R^3$ denotes the gravity vector. Furthermore, Equation (35)-(37) can be rewritten as:

$$
\begin{aligned}
V &= GS\dot{q} + GP_0V_0, \\
\dot{V} &= GS\dot{V} + Gad_{S\dot{q}}\Gamma V + Gad_{S\dot{q}}P_0V_0 + GP_0\dot{V}_0 \\
F &= G^T J\dot{V} + G^T ad_V^* JV + G^T P_t^T F_{n+1}, \\
\tau &= S^T F
\end{aligned}
\tag{38}
$$

where

$$
\begin{aligned}
&V = column[V_1, V_2, \cdots, V_n] \in R^{6n\times 1} \\
&F = column[F_1, F_2, \cdots, F_n] \in R^{6n\times 1} \\
&\dot{q} = column[\dot{q}_1, \dot{q}_2, \cdots, \dot{q}_n] \in R^{n\times 1} \\
&\tau = column[\dot{\tau}_1, \dot{\tau}_2, \cdots, \dot{\tau}_n] \in R^{n\times 1} \\
&P_0 = column[Ad_{f_{0,1}^{-1}}, 0_{6\times 6}, \cdots, 0_{6\times 6}] \in R^{6n\times 6} \\
&P_t^T = column[0_{6\times 6}, 0_{6\times 6}, \cdots, Ad^*_{f_{n,n+1}^{-1}}] \in R^{6n\times 6} \\
&S = diag[S_1, S_2, \cdots, S_n] \in R^{6n\times n} \\
&J = diag[J_1, J_2, \cdots, J_n] \in R^{6n\times 6n} \\
&ad_{S\dot{q}} = diag[-ad_{S_1\dot{q}_1}, \cdots, -ad_{S_n\dot{q}_n}] \in R^{6n\times 6n} \\
&ad_V^* = [-ad_{V_1}^*, \cdots, -ad_{V_n}^*] \in R^{6n\times 6n} \\
&G = I + \Gamma + \cdots + \Gamma^{n-1} \in R^{6n\times 6n}
\end{aligned}
$$

$$
\Gamma = \begin{bmatrix}
0_{6\times 6} & 0_{6\times 6} & \cdots & 0_{6\times 6} & 0_{6\times 6} \\
Ad_{f_{1,2}^{-1}} & 0_{6\times 6} & \cdots & 0_{6\times 6} & 0_{6\times 6} \\
0_{6\times 6} & Ad_{f_{2,3}^{-1}} & \cdots & 0_{6\times 6} & 0_{6\times 6} \\
\vdots & \vdots & \ddots & \vdots & 0_{6\times 6} \\
0_{6\times 6} & 0_{6\times 6} & \cdots & Ad_{f_{n-1,n}^{-1}} & 0_{6\times 6}
\end{bmatrix} \in R^{6n\times 6n}.
$$

Here, Γ is a nilpotent matrix [90]. Finally, Equation (34) can be rewritten as,

$$M(q)\ddot{q} + C(q, \dot{q})\dot{q} + \phi(q) + J_t^T(q)F_t = \tau \tag{39}$$

where $M(q) = S^T G^T JGS$

$$C(q, \dot{q}) = S^T G^T (JGad_{S\dot{q}}\Gamma + ad_V^* J)GS$$

$$\phi(q) = S^T G^T JGP_o\dot{V}_o$$

$$J_t(q) = P_t GS$$

The differential equation of motion of the proposed robotic manipulator is represented in Appendix.

CHAPTER V

NAVIGATION STRATEGY

The potential field methodology has been used extensively for manipulator path planning [19, 91, 92]. This method has been known as much faster solution than other heuristic algorithms, due to its computational efficiency. It can help robots to re-plan quickly with the time available for planning, as their knowledge of the terrain changes [40].

The basic concept behind the potential field method is its relatively simple. This method provides the resultant vector field of potential field vectors as a guiding path for a robot to reach the goal. A potential function is similar to the electrostatic potential and topological structure of the free space [39]. A goal and a set of obstacles are represented by an attractive pole and repulsive surfaces, respectively [91]. At robot's current posture, this method describes the workspace via the sum of a positive force attracted to the target and a negative force repulsed from objects. The sum of all forces exhibits the knowledge of the resultant direction and magnitude (speed) of a manipulator motion. This resultant vector generated by the artificial potential field is utilized as the control input to a robot.

In a manipulator path planning, an end-effector of a redundant robotic manipulator is assumed to be an ideal point. Robot has moved from the current robot's position (high potential point) toward a goal (low potential point) as a mapping form one vector into another vector. Let $P_c = [x_c \quad y_c \quad z_c]^T$ be the end-effector position of a redundant

manipulator in a three dimensional workspace. $P_g = [x_g \quad y_g \quad z_g]^T$ and $P_o = [x_o \quad y_o \quad z_o]^T$ are the positions of the goal and obstacles. The distance and angles between a goal and an end-effector are as follows:

$$d(P_g - P_c) = \sqrt{(x_g - x_c)^2 + (y_g - y_c)^2 + (z_g - z_c)^2} \tag{40}$$

$$\theta_x = \text{atan}\left(\frac{z_g - z_c}{y_g - y_c} \right) \tag{41}$$

$$\theta_y = \text{atan}\left(\frac{z_g - z_c}{y_g - y_c} \right) \tag{42}$$

$$\theta_z = \text{atan}\left(\frac{y_g - y_c}{x_g - x_c} \right) \tag{43}$$

Traditionally, the attractive potential is designed as a function of the relative distance between a robot and a stationary goal. It can be written as [91, 93],

$$U_{att}(q) = \frac{1}{2} \xi d^2 (P_g - P_c) \tag{44}$$

where ξ is a positive scaling factor. The following attractive force is calculated through the negative gradient of the attractive potential:

$$F_{att}(q) = -\nabla_q U_{att}(q) \tag{45}$$

Meanwhile, the construction of the repulsive potential, which is a function of either the relative positions or velocities between a robot and obstacles, would provide

free space into robot. In this study, we assume arbitrary convex obstacles and define the repulsive potential and its force as follows:

$$U_{rep}(q) = \begin{cases} \frac{1}{2}\eta\left(\frac{1}{d^2(P_g - P_o)} - \frac{1}{P_o}\right)^2 & ,if\ d(P_g - P_c) \le r \\ 0 & ,if\ d(P_g - P_c) > r \end{cases} \tag{46}$$

$$\begin{aligned} F_{rep}(q) &= -\nabla_q U_{rep}(q) \\ &= \begin{cases} \eta\left(\frac{1}{d(P_g - P_o)} - \frac{1}{r}\right)^2 \times \frac{1}{d^2(P_g - P_o)} \nabla_q d(P_g - P_o) & ,if\ d(P_g - P_o) \le r \\ 0 & ,if\ d(P_g - P_o) > r \end{cases} \end{aligned} \tag{47}$$

where *r* denotes the distance of influence of the obstacle.

However, the local minima problem in traditional potential field is important concern [40]. As a major drawback, it would lead robot not to escape and therefore causes the planner to fail [94]. In other hands, it makes a robot to a stable positioning before reaching its goal [40]. Especially, local minima can easily occur in a cluttered environment, subject to a local perspective of the robot environment.

In this study, I modified the traditional potential field to deal with the local minima [95]. It can be generated from the magnitude and direction in the same way as for the repulsive obstacle. However, one difference is that this function uses the modified axis angles ($\theta_x+90, \theta_y+90, \theta_z+90$) instead of the axis angle ($\theta_x, \theta_y, \theta_z$) of repulsive potential field. So, this weighted potential field points away from the center of the obstacle toward the direction of the tangent to the circle [96, 97, 98].

$$U_{\tan}(q) = \left\| U_{rep}(q) \right\| \times [\cos(\theta_x + pi/2), \cos(\theta_y + pi/2), \cos(\theta_z + pi/2)]^T \quad (48)$$

$$F_{\tan}(q) = -\nabla_q U_{\tan}(q) \quad (49)$$

So, the total force applied to the robot will be described as the following equation:

$$F_{total}(q) = F_{att}(q) + F_{rep}(q) + F_{\tan}(q) \quad (50)$$

This artificial potential field provides an end-effector of a robotic manipulator to move in the direction of this resultant force as in Equation (51),

$$\begin{aligned} F_{total}(q) &= -\nabla_q U_{att}(q) - \nabla_q U_{rep}(q) - \nabla_q U_{\tan}(q) \\ &= -\nabla_q (U_{att}(q) + U_{rep}(q) + U_{\tan}(q)) \end{aligned} \quad (51)$$

CHAPTER VI

CONTROL STRATEGY

In this study, we have considered a novel robust bio-inspired sliding mode control to achieve favorable tracking performance for the proposed robotic manipulators with uncertainties. To eliminate the chattering problem of the conventional Sliding Mode Control (SMC), we apply the Brain Emotional Learning Based Intelligent Control (BELBIC) to adaptively adjust the control input law in sliding mode control.

Dynamic Characteristic of Robotic Manipulator

In the presence of uncertainty and external disturbances, the dynamic equation of n-link manipulator can be expressed as the following vector form,

$$[M_0+\triangle M]\ddot{q}+(C_0+\triangle C)\dot{q}+[g_0+\triangle g]+\tau_d=u(t), \tag{52}$$

where $q,\dot{q},\ddot{q}\in R^{n\times 1}$ are position, velocity and acceleration vectors of joints, respectively. $M_0\in R^{n\times n}, C_0\in R^{n\times 1}, g_0\in R^{n\times 1}$ are the known parts of inertia matrix, coriolis/centrifugal force, and gravitational torque, respectively. $\triangle M\in R^{n\times n}, \triangle C\in R^{n\times 1}, \triangle g\in R^{n\times 1}$ are the unknown parts. $\tau_d\in R^{n\times 1}$ and $u\in R^{n\times 1}$ are the disturbance matrix and joint control inputs. Equation (52) can be rewritten as,

$$[M_0\ddot{q}+C_0\dot{q}+g_0]+[\triangle M\ddot{q}+\triangle C\dot{q}+\triangle g]+\tau_d=u(t). \tag{53}$$

If all uncertainty elements are assumed to be lumped, the dynamic model can be expressed as [50],

$$\ddot{q}=M_0^{-1}(u(t)-f_0-D(t)), \tag{54}$$

where $f_0=(C_0\dot{q}+g_0)$, $D(t)=(\triangle B\ddot{q}+\triangle C\dot{q}+\triangle g+\tau_d)$.

Conventional Sliding Mode Control

In sliding mode control design, the construction of the sliding surface (also called switching surface or sliding manifold) is very important. The intention of the switching control law is to keep the nonlinear plant's state trajectory along the boundaries of the control structure. This term means concerning back and force across the switching surface. The switch between two gain values, which are selected by the user-chosen rule at each instance, is the main factor to cause the chattering phenomena. Ideally, if infinitely fast switching were possible, the plant's state trajectories would lie on sliding surface for all subsequent times.

The sliding surface can be defined as follows,

$$s(t)=\dot{e}(t)+\alpha\cdot e(t),\ \ s(t)\in R^{n\times 1},\ \alpha\in R^{n\times n}, \tag{55}$$

where α_i and $e(t)$ are the coefficient matrix and the tracking position errors [46]. The tracking problem in this strategy can be achieved in two levels [50]. The first level is to keep the system trajectory on the sliding surface, *s(t)=0*. The other is to move along the sliding surface to the origin. To obtain this performance, the sliding surface should be asymptotically stable. That is to say, the system dynamics can track the desired trajectory with zero terminal error. It implies that the derivative of sliding surface is expressed as,

$$\dot{s}(t)=\ddot{e}(t)+\alpha\cdot\dot{e}(t)=\ddot{q}_d-M_0^{-1}(u(t)-f_0-D(t))+\alpha\cdot\dot{e}(t), \tag{56}$$

where $e(t)=q_d-q$.

Considering the nominal model with no uncertainty, its equivalent control input (in Figure 9) is expressed as:

$$u_n(t)=f_0+M_0[\ddot{q}_d+\alpha\cdot\dot{e}(t)]. \tag{57}$$

Furthermore, to compensate for the unpredictable perturbations resulting from the uncertainties, the following control input, $u_r(t)$, is considered [46, 47],

$$u_r(t)=K_r\cdot sign[s(t)],\quad K_r\in R^{n\times n}, \tag{58}$$

where K_r is diagonal matrix concerned with the upper bound of uncertainties. Finally, the total input vector for nonlinear uncertain system can be represented as (in Figure 11):

$$u(t)=u_n(t)+u_r(t)=f_0+M_0[\ddot{q}_d+\alpha\cdot\dot{e}(t)]+K_r\cdot sign[s(t)] \tag{59}$$

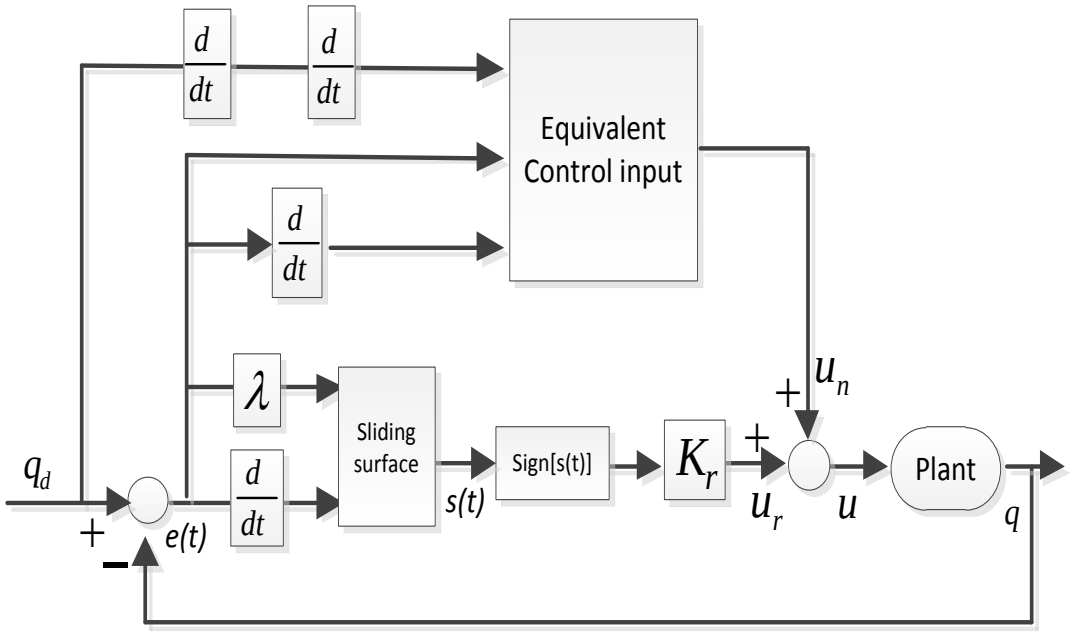

Figure 11. Block diagram of conventional SMC strategy

Brain Limbic System Control

The human brain is composed of many lobes supporting a variety of emotional processing function (in Figure 12). In a brain structure, brain limbic system is intended to obtain appropriate stimuli from relevant signals through brain emotional learning processes. Regarding the emotional processing mechanism, important parts and corresponding functions in the brain limbic system are as follows [57]:

- Amygdala: the role of mapping from the sensory stimuli to emotional response.
- Orbitofrontal Cortex: the role of inhibiting the inappropriate links as a goal change.
- Sensory Cortex: the role of generating the sensed input via the incoming sensory stimuli.
- Thalamus: the role of the communicating between sensed inputs and the others of BLS.

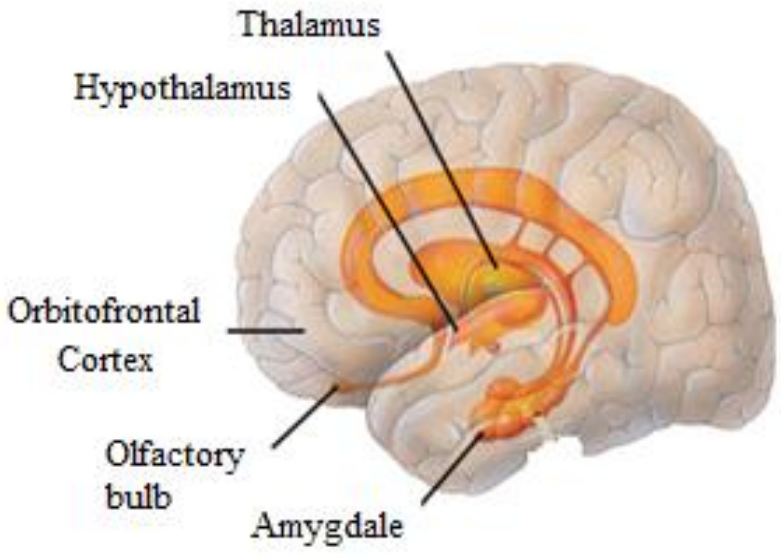

Figure 12. The schematic of the human brain

A mathematical model of brain limbic system process, developed by Moren and Balkenius, is used in this study (in Figure 13). The sensory input (SI) and the emotional signal (EC) are designed by considering the objective of control. The difference between SI and EC, MO, is defined as the output of the controller.

$$MO = \sum_i` A_i - \sum_i` OC_i \tag{60}$$

where the subscript i represents the i^{th} sensing flow. The output signals of the Amygdala and the OFC with respect to the sensory inputs (SI) and emotional cue (EC), denoted by G_A and G_{OC}, are explained as displayed in Equation (61)-(64), respectively. ΔG_{A_i} and ΔG_{OC_i} are defined as the incremental adjustments of Amygdala and the OFC signal, respectively. According to the objective of control, the SI signals and the EC signals are designated as follows.

$$A_i = G_A \cdot SI_i \tag{61}$$

$$OC_i = G_{OC_i} \cdot SI_i \tag{62}$$

$$\Delta G_{A_i} = \alpha \cdot SI_i \cdot \max\left(0, \mathrm{EC}_i - \sum_i A_i\right) \tag{63}$$

$$\Delta G_{OC_i} = \beta \cdot SI_i \left(\sum_i A_i - \sum_i OC_i - \mathrm{EC}_i\right) \tag{64}$$

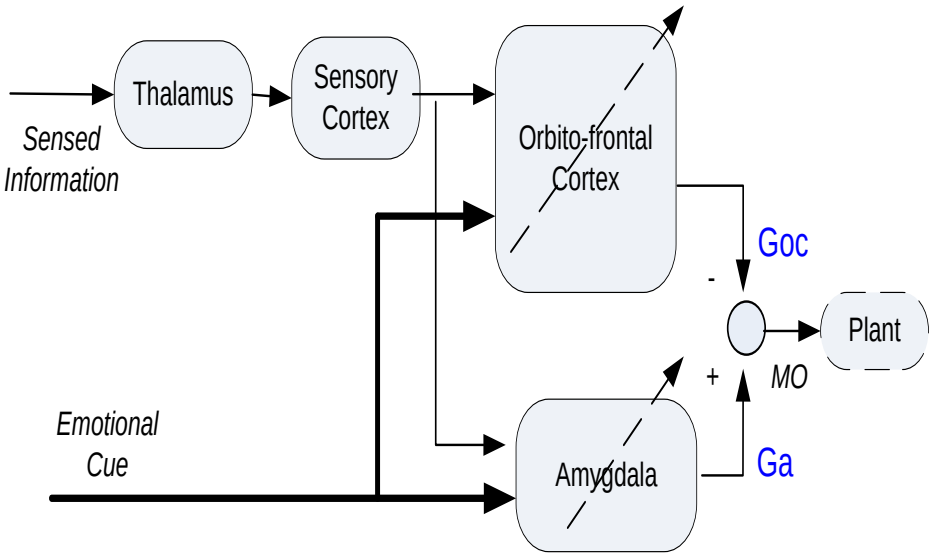

Figure 13. A computational model of BLS [57, 63]

Here α and β are the learning rate, selectable between 0 (no learning) and 1 (instant adaptation). In practice, they are set at a fairly low value. In the learning process, the learning rate α is associated with the difference among the strength of the emotional cue (EC), the strength of stimulus signal (SI), and the current output of the Amygdala nodes. β is also the learning rate to reflect a faster learning rate than that of Amygdala.

Proposed Control Strategy

The goal of our study is to develop a novel robust sliding mode control strategy, which replaces the term $K_r\, sign$[s(t)] in Equation (58) with a new control input term. This term in conventional sliding mode control leads to the chattering phenomena while` tracking high speed trajectories. Moreover, it is difficult to select the proper factor (K_r) based on the bounds of uncertainties. The on-line computed parameters achieve favorable system robustness regarding parameter uncertainties and external disturbances.

Therefore, in this paper, we design the new adaptive control input term, u_p, to deal with uncertainty and external disturbances, based on brain limbic system control. The design of proper control input depends on online estimated uncertainties, instead of selection of the bound uncertainties. The structure of our approach is displayed in Figure 14.

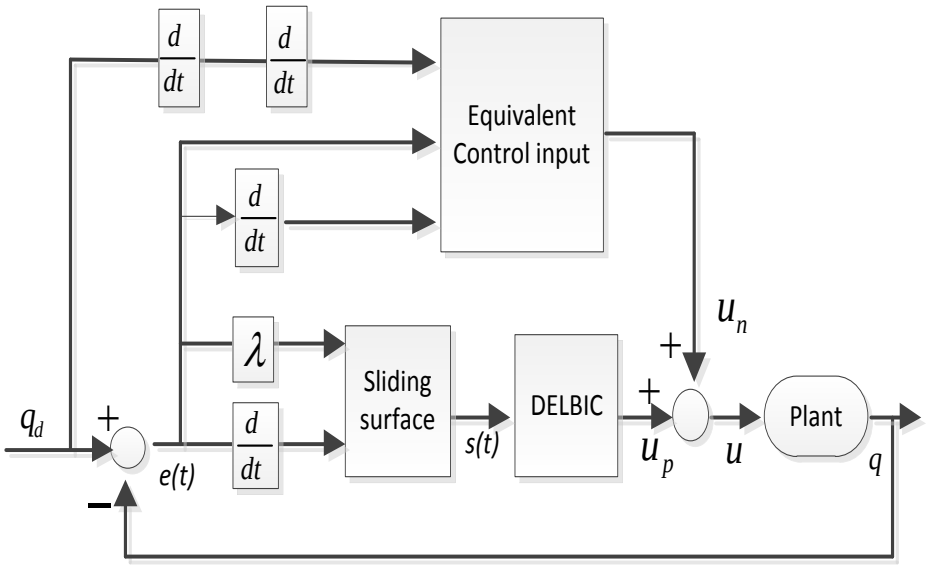

Figure 14. Block diagram of the proposed SMC strategy

In addition to the equivalent control inputs, the additional control input improves the performance of the controller. Instead of $K_r \cdot sign$[s(t)] in Equation (58), the brain limbic system controller plays an important role of generating control inputs. It is to reduce chattering reduction in high speed dynamics. The weighted sliding surface error between the current sliding surface, $s_{i,r}(t)$, and the previous sliding surface, $s_{i,r-1}(t)$, at each link is used to generate *SI*. The *EC* function is designated as the summation of the weighted *SI*, the weighted error of joint trajectories, and the weighted control input to the plant, u_p. These two variables are defined as follows:

$$\mathrm{SI}_i = \mu_i (s_{i,r}(t) - s_{i,r-1}(t)), \tag{65}$$

$$\mathrm{EC}_i = \gamma_i \, SI_i + \delta_i u_{i,p}, \tag{66}$$

$$\gamma_i = \sqrt{\sum (x_i - x_{i-1})^2}, \ \mu_i > 0, \ \delta_i \geq 0, \ i = 1,2,\cdots,n. \tag{67}$$

However, in the case of the target position, the BLS output might not converge to zero. So, control output is defined as the integral of the weighted multiplication of SI and MO ($-1 \leq \int (SI \times MO) dt \leq 1$), as follows [62], [63]:

$$u_p = K_m \int (SI \times MO) dt, \tag{68}$$

where K_m is a diagonal control gain matrix. Therefore, the total input vector for nonlinear uncertain system in our study can be represented as:

$$u(t) = f_0 + M_0[\ddot{q}_d + \alpha \cdot \dot{e}(t)] + K_m \int (SI \times MO) dt. \tag{69}$$

Lyapunov Stability

In this study, Lyapunov stability analysis is employed to prove and to evaluate the existence of sliding mode [48, 99]. In *n*-inputs/*n*-outputs system of the Equation (58), each component *i* of the output vector (n×1) may be assigned its own sliding manifold independently. We can address the sliding manifolds and the time derivative in the Equation (55)-(56) as [48],

$$s_i(t)=\dot{e}_i(t)+\alpha_i\cdot e_i(t), \tag{70}$$

$$\dot{s}_i(t)=\ddot{e}_i(t)+\alpha_i\cdot \dot{e}_i(t), \tag{71}$$

where $s_i(t)\in R,\ \alpha_i\in R,\ i=1,\cdots,n.$ Each component of the system can be rewritten as,

$$\ddot{q}_i(t)=[M_0^{-1}(u(t)-f_0-D(t))]_i=\frac{1}{m_{i,i}}[u_i-f_{0_i}-D_i-\sum_{j=1,i\neq j}^{n} m_{i,j}\ddot{q}_j]. \tag{72}$$

The Lyapunov function and its time derivative for each component can be chosen as:

$$\begin{aligned} V_i(t) &= \frac{1}{2}s_i(t)s_i(t) > 0, \\ \dot{V}_i(t) &= s_i(t)\dot{s}_i(t) \le 0. \end{aligned} \tag{73}$$

Then, a combination of Equations (70)-(73) becomes [48],

$$\begin{aligned} \dot{V}_i(t) &= s_i(t)[\alpha_i\dot{e}_i(t)+\ddot{q}_{d_i}-\frac{1}{m_{i,i}}(u_i-f_{0_i}-D_i-\sum_{j=1,i\neq j}^{n} m_{i,j}\ddot{q}_j)] \\ &= -s_i(t)\frac{1}{m_{i,i}}u_i+s_i(t)[\alpha_i\dot{e}_i(t)+\ddot{q}_{d_i}+\frac{1}{m_{i,i}}(f_{0_i}+D_i+\sum_{j=1,i\neq j}^{n} m_{i,j}\ddot{q}_j)] \\ &\le -s_i(t)\frac{1}{m_{i,i}}u_i+|s_i(t)|[\alpha_i|\dot{e}_i(t)|+|\ddot{q}_{d_i}|+\frac{1}{m_{i,i}}(|f_{0_i}|+|D_i|+\sum_{j=1,i\neq j}^{n} m_{i,j}|\ddot{q}_j|)] \end{aligned} \tag{74}$$

Therefore, the proper SMC law, which guarantees for the existence of the sliding manifold, is as follows,

$$-s_i(t)\frac{1}{m_{i,i}}u_i+|s_i(t)|[\alpha_i|\dot{e}_i(t)|+|\ddot{q}_{d_i}|+\frac{1}{m_{i,i}}(|f_{0_i}|+|D_i|+\sum_{j=1,i\neq j}^{n}m_{i,j}|\ddot{q}_j|)]\leq 0, \qquad (75)$$

The controller gain (k_{m_i}) is determined from the stability analysis, as shown in Equation (76).

$$\text{Case 1: } s_i(t)>0;\ k_{m_i}\geq m_{i,i}[\alpha_i|\dot{e}_i(t)|+|\ddot{q}_{d_i}|]+[(|f_{0_i}|+|D_i|+\sum_{j=1,i\neq j}^{n}m_{i,j}|\ddot{q}_j|)]-u_{n_i}, \qquad (76)$$

$$\text{Case 2: } s_i(t)<0;\ k_{m_i}\geq -m_{i,i}[\alpha_i|\dot{e}_i(t)|+|\ddot{q}_{d_i}|]-[(|f_{0_i}|+|D_i|+\sum_{j=1,i\neq j}^{n}m_{i,j}|\ddot{q}_j|)]-u_{n_i}.$$

A condition of the control gain for the existence of the sliding mode is determined subject to the sign of the error of the sliding mode.

An Example of the 3 DOFs Link

The dynamic equation of a single link can be expressed in the following vector form,

$$\dot{x}=f(x)+g_1(x)u_1+g_2(x)u_2+g_3(x)u_3,\ \mathrm{x}\in R^3, u_i\in R,\ i=1,2,3,$$

where $s_i=\sin(x_i),\ c_i=\cos(x_i), s(2x_i)=\sin(2x_i),\ c(2x_i)=\cos(2x_i),$

$$f(x)=[\dot{x}_1,\dot{x}_2,\dot{x}_3,\dot{x}_4,\dot{x}_5,\dot{x}_6], \dot{x}_1=x_2, \dot{x}_3=x_4, \dot{x}_5=x_6,$$

$$\dot{x}_2=[\frac{0.5L_3m_3(s_3\dot{x}_6+c_3x_5x_5)-g(m_1+m_2+m_3)x_1}{m_1+m_2+m_3}], \qquad (77)$$

$$\dot{x}_4=[\frac{0.5(m_3x_2s_3(2L_2+L_3s_3)+c_3x_4(2L_2L_3m_3+c_3L_3m_3s_5)x_4+0.5g(L_2L_3m_3c_3)x_4x_6}{I_{z2}+L_2L_2m_3+I_{z3}c_3c_3+L_2L_3m_3s_3+(I_{x3}+0.25L_2L_2m_3)s_3s_3}],$$

$$\dot{x}_6=[\frac{\frac{1}{2}m_3(L_3s_3\dot{x}_6-(L_3c_3x_6+2x_2s_3)\dot{x}_2)-\frac{1}{2}c_3x_4(L_2L_2m_3+\frac{1}{2}L_2L_3m_3s_3)-\frac{1}{2}L_3m_3(x_2+gs_3)}{I_{y3}+0.25L_3L_3m_3}].$$

In this study, the tracking control is implemented to identify the effectiveness and robustness of our control approach. Under modeling uncertainty and external disturbance torques, the tracking performance of the suggested robust control strategy for a given reference trajectories (in Figure 15) is investigated and compared to that of conventional sliding mode control strategy. To investigate the effectiveness of learning process in our approach, each of the three joints tracks 3 cycles of a given trajectories over a 2.5 sec.

In our simulation, the two parameters (length and mass) have the modelling uncertainty into the maximum 10% variations of nominal values (in [100]). The fixed slope of sliding surface is set at 5 for all joint variables. External disturbances at each joint are assumed by,

$$\begin{aligned} T_{d1}(t)&=2\sin(t)+0.2,\\ T_{d2}(t)&=\sin(t)+0.1,\\ T_{d3}(t)&=0.5\sin(t)+0.1, \end{aligned} \qquad \text{at t=time.} \qquad (78)$$

From the simulation results, it is concluded that our robust sliding mode control approach showed effective performance for each of the three joints. Under same values of both K_r in Equation (58) and K_m in Equation (68), we compared both U_r

($=K_r \cdot \text{sign}[s(t)]$) and $U_p (= K_m \int (SI \times MO) dt)$, which compensate the tracking errors against uncertainties and external disturbances, respectively.

In Figure 16, we observed that the robust sliding mode control with brain limbic system control strategy provides less tracking errors than conventional sliding mode control strategy. Even through a relatively larger initial errors are existed in our approach, it could move along with given reference trajectories through learning process to learn some gains in brain limbic system. We found that trajectory errors of each joint converged to zero, as our system tracks given trajectories. However, each joint controlled by conventional sliding model control approach has not properly converged to a zero error. In Figure 17, the simulation results showed that our control strategy has less chattering, compare to that of conventional sliding mode control. Our strategy only commands the large control inputs when the each joint faces to the changing direction of each trajectories at t = 1.25, 2.5, 3.75, 5, 6.25 sec.

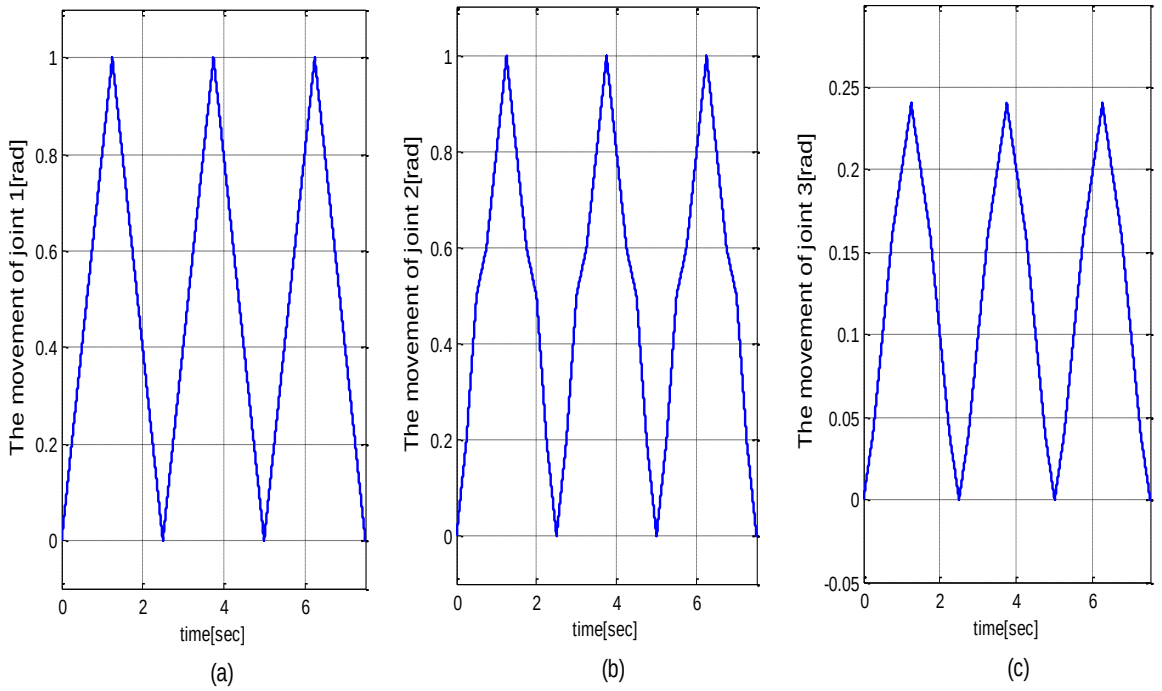

Figure 15. Given trajectories of each joint (a) joint 1 (b) joint 2 (c) joint 3

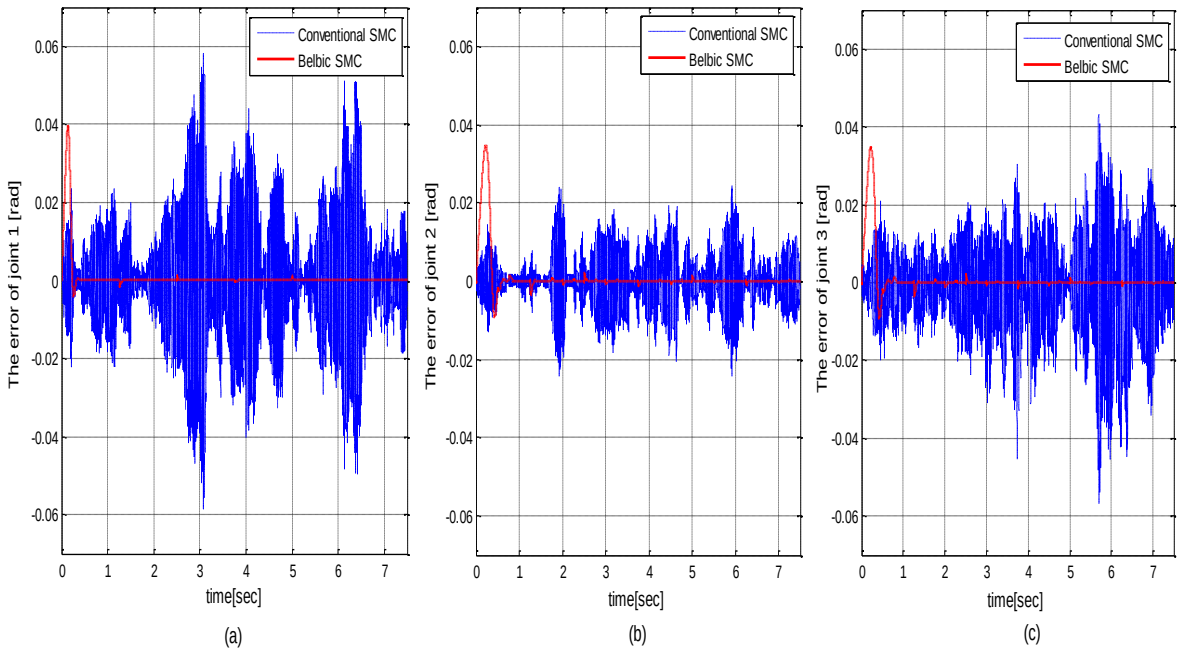

Figure 16. The tracking errors of each joint (a) joint 1 (b) joint 2 (c) joint 3

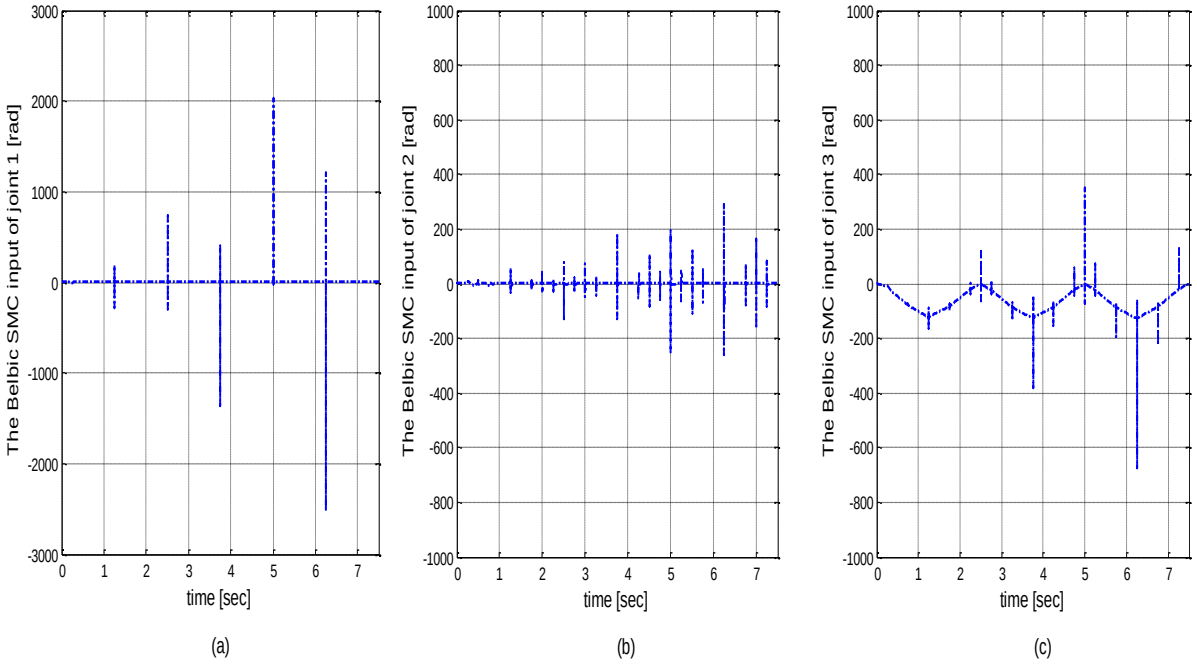

Figure 17. The control input for uncertainties and unexpected external torque (a) joint 1 (b) joint 2 (c) joint 3

CHAPTER VII

RESULTS

In this Chapter, the simulation results demonstrate the effectiveness of the proposed robotic manipulator and bio-inspired sliding mode control strategy in small and constrained workspace, discussed in previous Chapters.

Reachable Workspace

In this Chapter, the reachable workspaces of both the proposed link and the manipulator made up of this type of a link are investigated to identify the effectiveness of our design strategy. This design is compared to a serial-chained with three JPL serpentine 2-DOFs links and an end-effector of on the same link's length [101].

Figure 18 represents the reachable workspace of the 3-DOFs link, as a function of the motion of the individual joints. The reachable workspace of the developed link with only y-axis rotational motion is shown in Figure 18a. Its workspace is a sinusoidal curve, such as in the case of a general 1 DOF link. In Figure 18b, the second subsystem plays a role in rotating the sinusoidal curve (in Figure 18a) around the z axis. This workspace is similar in shape to a hemispherical shell. In additions, the first subsystem embedded in the link contributes to the workspace of the two subsystems to be extended along the z direction. Eventually, the reachable workspace of our link is changed from a hemispheric shape to a cylindrical one.

As shown in Figure 19, our 3-DOFs link has a symmetric workspace, while a 2-

DOFs serpentine-type link [101] is asymmetric. The symmetric shape is very beneficial for a manipulator to function in constrained environments, to deal with a variety of constrained directions. Particularly, in small and constrained environment, the link's variable length is a good option to reconfigure efficiently.

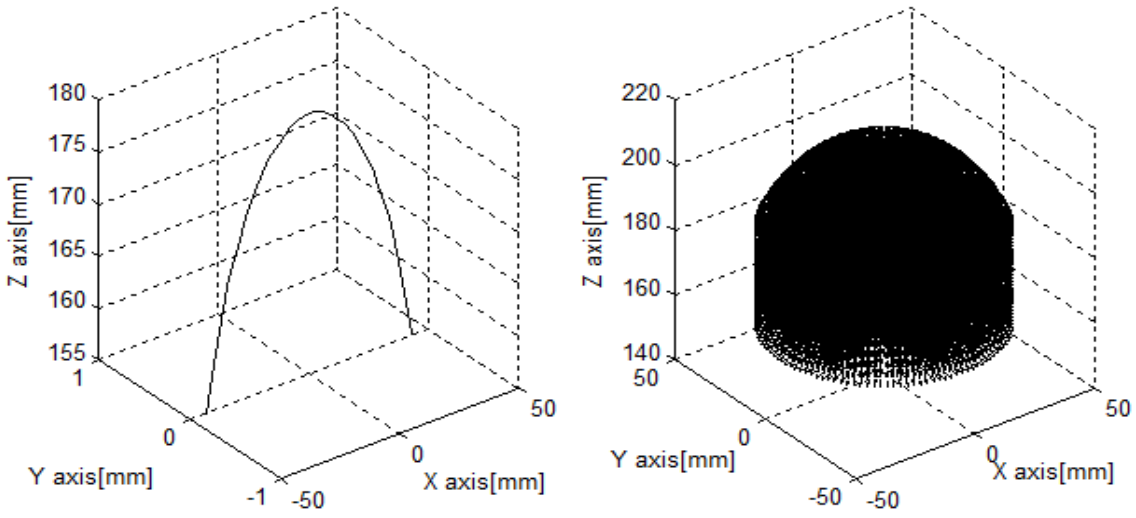

(a) (b)

Figure 18. The workspace analysis (a) a 1DOF general link (b) the proposed 3DOFs link

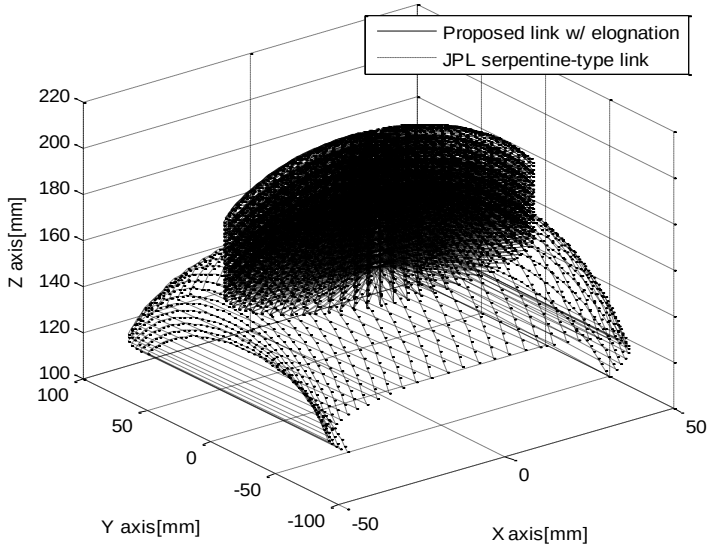

Figure 19. The workspace comparison

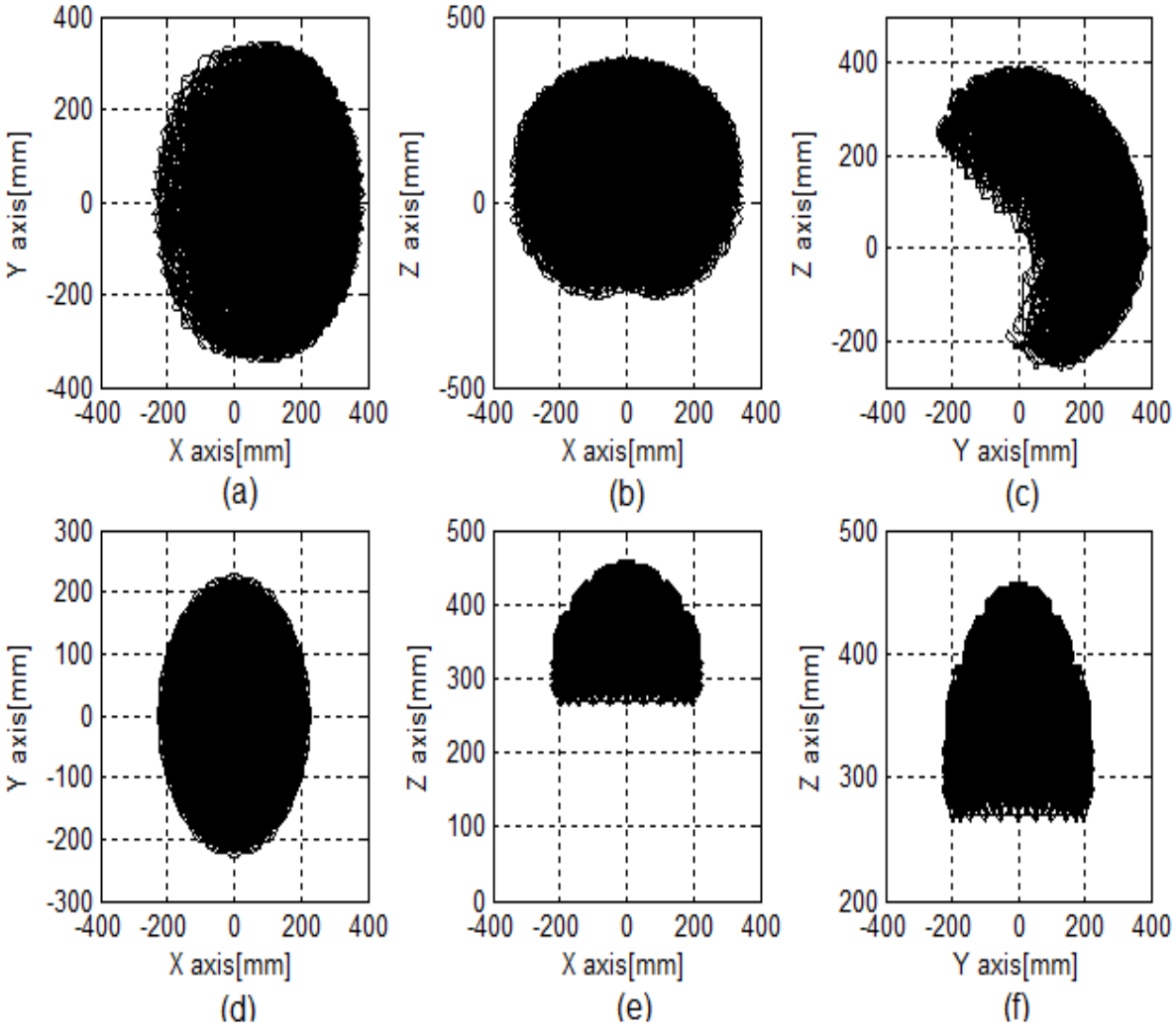

Figure 20. 2-D images of the reachable workspace (a)-(c) a serpentine manipulator (d)-(f) the proposed manipulator

Figure 20 represents all the projected 2-D images of the reachable workspace, compared to those of the 7 DOFs serpentine manipulator. Figure 20a and Figure 20d illustrate the projected x-y images of the manipulator workspace. Both reachable workspaces are similar and elliptic, but the only proposed manipulator has complete symmetry around the z-axis. So, our robotic manipulator can efficiently complete the

required missions based on its symmetrical workspace. Even though the reachable workspace of our manipulator is smaller to that of the JPL serpentine manipulator, it is very beneficial to reconfigure free motion in dealing with constrained the x-y type planes. As can be seen in Figure 20c and Figure 20f, the projected y-z plane workspace of our manipulator is relatively smaller but generally symmetric compared to that of the JPL serpentine manipulator. Regarding constraints in y-z plane, our robotic manipulator can have more versatile motion, compared to a JPL serpentine manipulator.

Case Study

To demonstrate the effectiveness of the proposed robotic system and robust nonlinear control strategy, a path planning and its tracking simulation of the proposed manipulator in constrained setting are investigated. The equation of motion of the utilized robot is given in the Appendix. Based on the knowledge of Chapter 7, we designed a robust sliding mode controller with brain limbic system control, and compared its results with those of conventional sliding mode control.

In our study, ADAMS (Automatic Dynamic Analysis of Mechanical Systems) is used for construction of the robot's graphical model and robot's working environment, as shown in Figure 21. Through using a graphical dynamic model, we can provide simulation tests of a dynamic model without installing hardware experiments. However, to add realism, we assume IR sensors with 10 mm sensing range on each link to measure the shortest distance between obstacles and the exterior of each link.

Robot's initial and goal posture in three dimensions are set to (0 mm, 0 mm, 400 mm, 0 radian, 0 radian, 0 radian) and (40 mm, 50 mm, 450 mm, 0.2 radian, 0.4 radian, 0.25 radian), respectively. The fourteen parameters that are each link's length and mass include the modelling uncertainty up to a maximum 5% of nominal values. The fixed slope of sliding surface is set at 10 for all joint variables. External disturbances at the i^{th} joint, denoted by $T_{di}(t)$, are given as in equation (79),

$$
\begin{aligned}
&T_{d1}(t)=2t\sin(5t)+0.01,\\
&T_{d2}(t)=t\sin(t)rand(0,1),\\
&T_{d3}(t)=t\sin(5t)rand(0,1)+0.01,\\
&T_{d4}(t)=2t\sin(5t)+0.01,\\
&T_{d5}(t)=t\sin(t)rand(0,1)+0.01,\\
&T_{d6}(t)=0.5t\sin(5t)rand(0,1)+0.01,\\
&T_{d7}(t)=0.5t\sin(5t)rand(0,1)+0.01,
\end{aligned}
\qquad \text{at t = time} \qquad (79)
$$

In our simulation, a potential field method provides the robot with a free path to track. The resultant path subject to our map settings is shown in Figure 22. During 0.2 sec ~ 0.5sec, our proposed robot re-calculates quickly to avoid the obstacles. At (x, y, x) = (5~15mm, 5~20mm, 410~420mm), we can see an oscillated path that is not smooth. While the manipulator approaches an obstacle, the obstacle is required to exert an arbitrarily large repulsive potential [21].

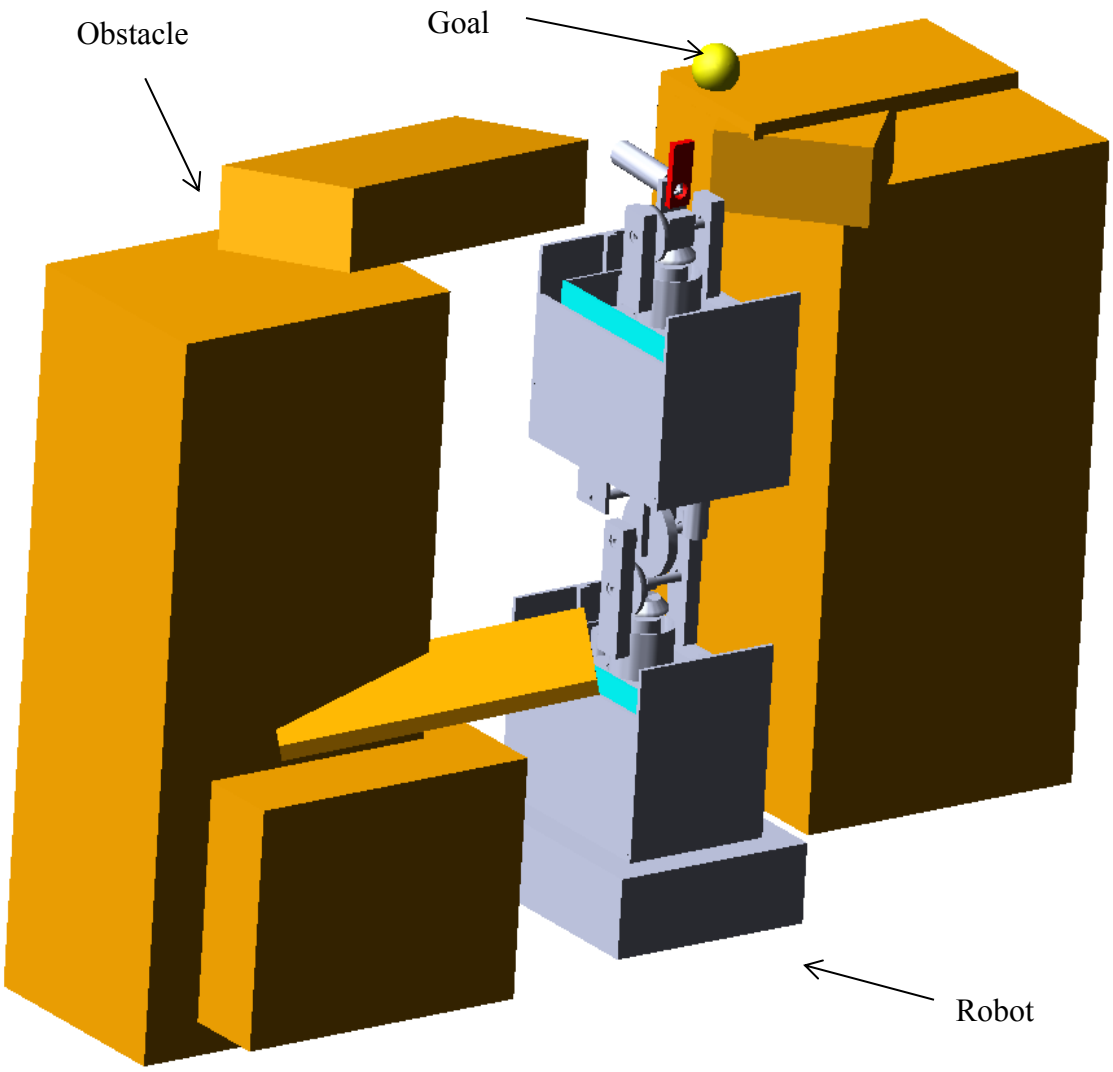

Figure 21. Robotic manipulator and obstacles in ADAMS

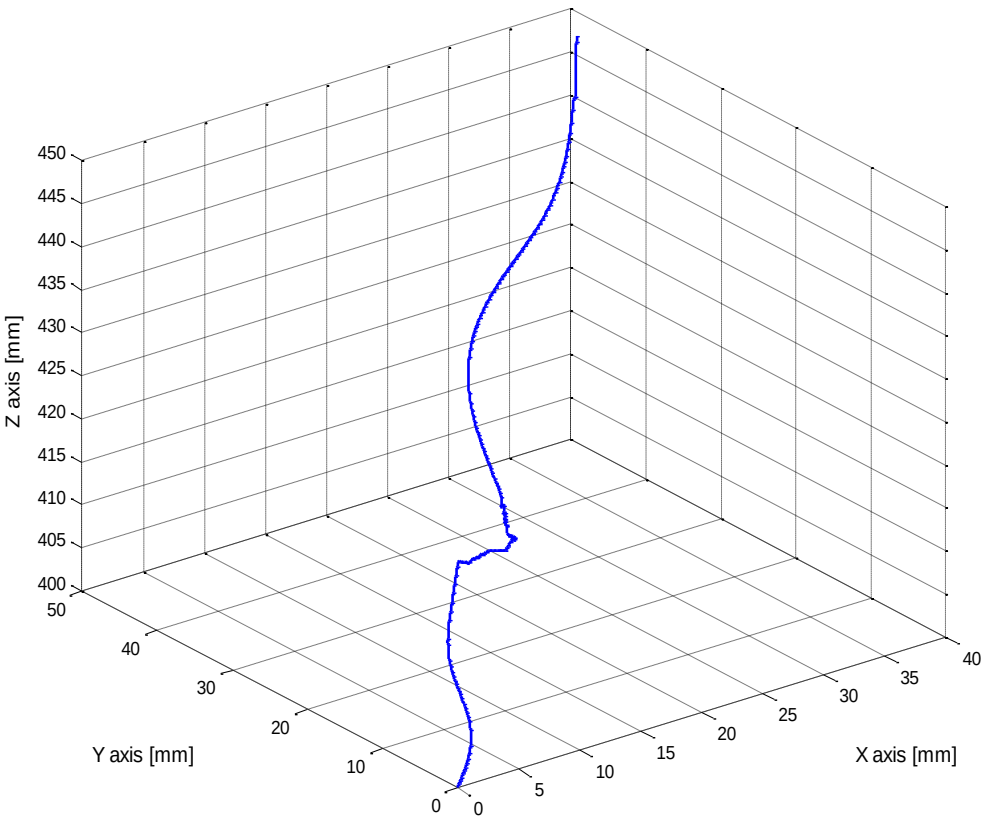

Figure 22.Generated path

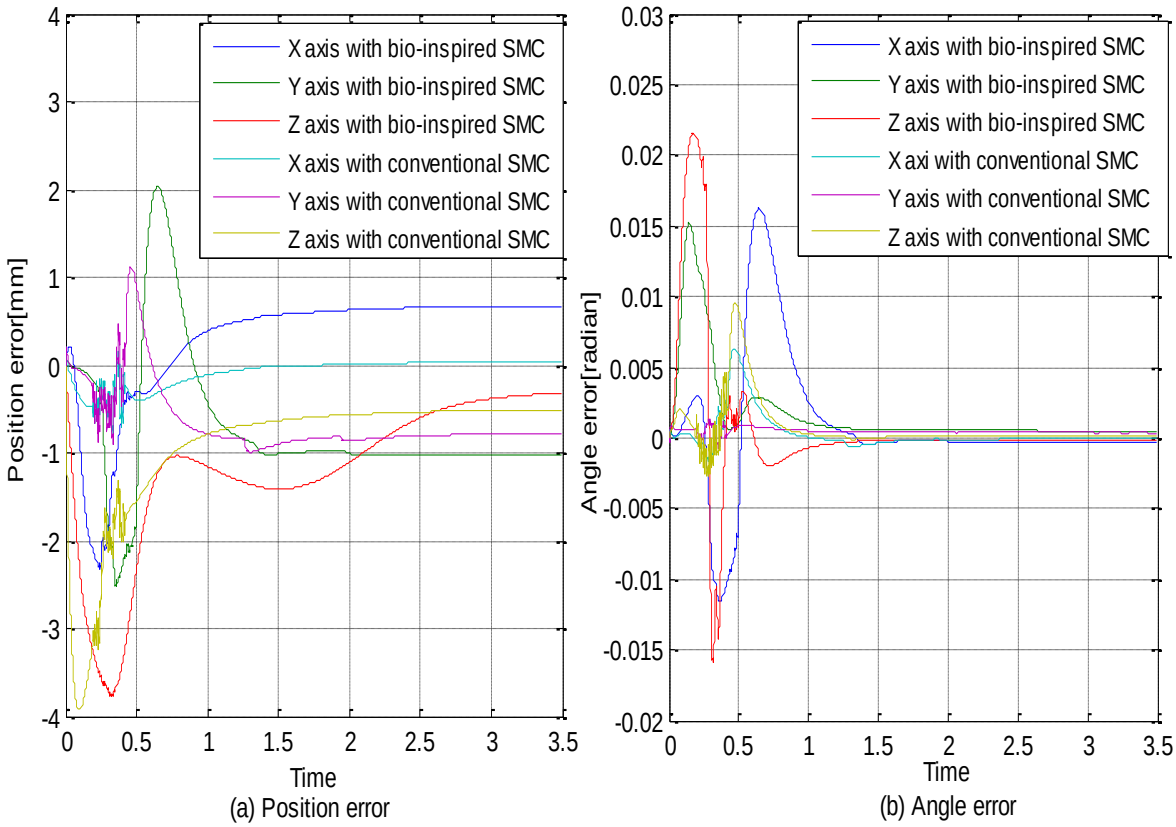

Figure 23. Trajectory errors (a) position error (b) angle error

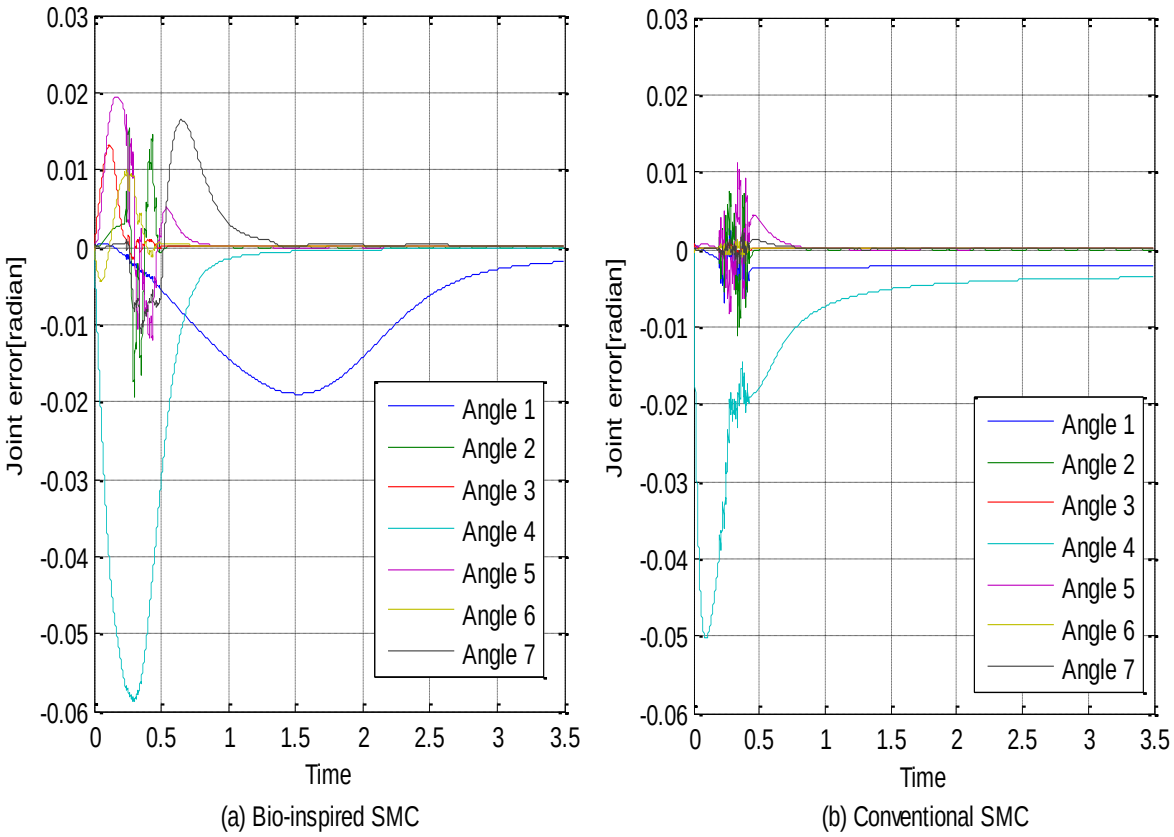

Figure 24. Joint error (a) bio-inspired SMC (b) conventional SMC

In Figure 23 and Figure 24, we observed that the robust sliding mode control with brain limbic system control strategy provides less tracking errors similar to that of conventional sliding mode control strategy. Even through relatively larger initial errors exist in our approach, it could move along with given reference trajectories through learning process to learn the gains in the brain limbic system algorithm. However, a conventional SMC has a high frequency chattering phenomenon around the expected collision area, but our control strategy provides less chattering. During 0.2 sec ~ 0.5 sec, our strategy strongly functions to adjust the large control inputs when the each joint must change the direction of its trajectory.

Also, we found that both control strategies fail to converge to zero error, as our system tracks generated trajectories. Because a relatively larger random external disturbance are assumed at each joint, our system has constant error after it reaches the surface area (4 mm ranged from the center of a goal) of a goal [46].

In our results, speed trajectories are not very high, compared to the trajectory speed of the previous example in Chapter 6. Because the robot meets the complex map environment and has small reachable workspace, our robot would move slowly. So, both control strategies are supposed to be good in this simulation setting. However, if the number of DOFs of our system increases or trajectories' speed is increasing, our controller will show the good performance, compared to conventional SMC.

CHAPTER VIII

CONCLUSION AND FUTURE STUDIES

Summary of Concluding Remarks

In this dissertation, we discuss an implementation of design, control and motion planning for a novel extendable modular redundant robotic manipulator.

The design of a new modular reconfigurable robotic manipulator, developed for dexterous motion in constrained setting, is investigated. To alleviate its structural weakness that they meet in small or complex environment, multi-DOFs links including controlling the link's length is developed. A variable length has an important role in extending the reachable workspace, compared to the fixed length of links. Furthermore, the symmetrical reachable workspace of our manipulator leads to an efficient reconfiguration for performing the required missions. Design optimization for conflicting multiple-objectives that have to be addressed simultaneously is investigated. The singularity and dexterous manipulability of the designed manipulator are investigated.

The inverse kinematic solution of the proposed redundant manipulator is resolved by redundancy resolution with obstacle collision avoidance approach. The potential field is considered to re-plan quickly, as the knowledge of the terrain changes. In this study, a combination of obstacle collision avoidance approach and potential field methods provides all joints' trajectory reference to our robot.

Also, we developed a novel robust sliding mode controller with brain limbic system control strategy. To eliminate the chattering problem of the conventional sliding mode control, we apply the Brain Emotional Learning Based Intelligent Control (BELBIC) to adaptively adjust the control input law in sliding mode control. The on-line computed parameters achieve favorable system robustness regarding parameter uncertainties and external disturbances. Through an analysis of Lyapunov stability, the condition of the existence of a sliding mode is investigated. In an example of the 3 DOFs link, the knowledge gained from the simulation results shows that our approach achieves the desired performance for tracking reference trajectories of our developed modular multi-DOF link.

Lastly, the simulation results show that our control strategy adaptively compensates against parameter uncertainties and external disturbances. Even though initial joint errors in our control strategy are relatively larger than those in a conventional sliding mode control, it leads to less chattering phenomenon when tracking high speed trajectories. As compared to the results of a conventional sliding mode control, the applied learning process provides the effectiveness of tracking high speed trajectories with less tracking errors.

Future Research

Design and control frameworks of the redundant modular robotic manipulator addressed in this dissertation have been investigated numerically. Although useful for design guidelines, further research needs experimental studies to demonstrate the effectiveness of the proposed methodologies.

Furthermore, it is recommended that the proposed control method should be implemented with parameter tuning techniques. The more complicated a system, the more burdensome the efforts to find optimal control parameters in our control strategy.

Lastly, even though the proposed robotic manipulator has the role of enlarging reachable workspace, it would perhaps be somewhat burdensome to control the system due to increased number of control variables. In future work, we will consider a distributed control strategy to have fewer side effects in this regard.

REFERENCES

[1] B. Davies, A review of robotics in surgery, *Proceeding of the Institution of Mechanical Engineers, Part H: Journal of Engineering in Medicine*, 214(1), 129-140(2000).

[2] J. Decuir, O. Kozuki, V. Matsuda, and J. Piazza, A friendly face in robotics: sony's AIBO entertainment robot as an educational tool, *Computers in Entertainment*, 2(2), 1-4(2004).

[3] A. Wolf, H. Choset, B. Brown, and R. Casciola, Design and control of a mobile hyper-redundant urban search and rescue robot, *Advanced Robotics*, 19, 221-248(2005).

[4] E. Shammas, A. Wolf, and H. Choset, Three degrees-of-freedom joint for spatial hyper-redundant robots, *Mechanism and Machine Theory*, 41(2), 170–190(2006).

[5] G. Chirikjian and J. Burdick, Kinematically optimal hyper-redundant manipulator configurations, *IEEE Transactions on Robotics and Automation*, 11, 794–806 (1995).

[6] G. Chirikjian and J. Burdick, A modal approach to hyper-redundant manipulator kinematics, *IEEE Transactions on Robotics and Automation*, 10, 343–354(1994).

[7] M. Yim, *Locomotion with a unit modular reconfigurable robot*, Dissertation, Stanford University, 1994.

[8] G. Haith, H. Thomas, and A. Wright, A serpentine robot for planetary and asteroid surface exploration, *Oral presentation at the Fourth IAA International Conference on Low-Cost Planetary Missions*, Laurel, MD, May 2000.

[9] H. Ikeda, N. Takanashi, *Joint assembly movable like a human arm*, US Patent 4, 683-406, July 1987.

[10] E. Paljug, T. Ohm, S. Hayati, The JPL serpentine robot: a 12-DOF system for inspection, *in Proceedings of IEEE Conference on Robotics and Automation*, 3, 3143–3148, 1995.

[11] S. Hirose, *Biologically Inspired Robots: Snake-like Locomotors and Manipulators*, Oxford University Press, 1993.

[12] R. Dubey, J. Euler, and S. Babock, An efficient gradient projection optimization scheme for a seven-degree-of-freedom redundant robot with spherical wrist, *in Proceedings of IEEE Conference on Robotics and Automation*, Sacramento, 28-36, Philadelphia, PA, 1988.

[13] O. Egeland, Task-space tracking with redundant manipulators, *IEEE Journal of Robotics and Automation*, RA-3(1987).

[14] L. Sciavicco and B. Siciliano, A solution algorithm to the inverse kinematic problem for redundant manipulators, *IEEE Journal of Robotics and Automation*, 4(4), 403- 410(1988).

[15] Y. Nakamura and H. Hanafusa, Inverse kinematic solutions with singularity robustness for manipulator control, *ASME Journal of Dynamic Systems, Measurement, and Control*, 108, 163-171(1986).

[16] H. Mark and T. Robert, Reducing flexible base vibrations through local redundancy resolution, *Journal of Robotic Systems*, 12(11), 767–779(1995).

[17] J. Hollerbach and S. Ki, Redundancy resolution of manipulators through torque optimization, *IEEE Journal of Robotics and Automation*, 3(4), 308- 316(1987).

[18] L. Alain, Automatic supervisory control of the configuration and behavior of multi-body mechanisms, *IEEE Transactions of systems, Man, and Cybernetics*, SMc-7(1977).

[19] O. Khatib, Real-time obstacle avoidance for manipulators and mobile robots, *International Journal of Robotics Research*, 5(1), 190-198(1986).

[20] J. Baillieul, J. Hollerbach, and R. Brockett, Programming and control of kinematically redundant manipulators, *Proceedings of the 23rd IEEE Conference on Decision and Control*, Las Vegas, NV, 768-774, 1984.

[21] Y. Umetani and K. Yoshida, Workspace and manipulability analysis of space manipulator, *Transaction of the Society of Instrument and Control Engineers*, E, 1-8(2001).

[22] T. Yoshikawa, Manipulability and redundancy control of robotic mechanisms, *Proceedings of the IEEE International Conference on Robotics and Automation*, St. Louis, MO, USA, 1004-1009(1985).

[23] J. O. Kim and K. Khosla, Dexterity measures for design and control of manipulators, *Proceedings of the IEEE/RSJ International Conference on Intelligent Robotics and Systems*, November 3-5, Osaka, Japan, 758-763(1991).

[24] C. Gosselin, and J. Angeles, Singularity analysis of closed-loop kinematic chains, *IEEE Transaction on Robotics and Automation*, 6, 281-290(1990).

[25] J. Salisbury and J. Craig, Articulated hands: force control and kinematic issues, *International Journal of Robotics Research 1(4),* 4-17(1982).

[26] C. Klein and B. Blaho, Dexterity measures for the design and control of kinematically redundant manipulators, *International Journal of Robotics Research,* 6, 72-83 (1987).

[27] R. Murray, Z. Li, and S. Sastry, *A Mathematical Introduction to Robotic Manipulation*, CRC Press, 1994.

[28] P. Chiacchio, S. Chiaverini, L. Sciavicco, and B. Siciliano, Global task space manipulability ellipsoids for multiple-arm systems, *IEEE Transaction on Robotics and Automation*, 7, 678-685 (1991).

[29] P. Chiacchio, A new dynamic manipulability ellipsoid for redundant manipulators, *Robotica*, 18, 381–387(2000).

[30] J. Hollerbach, A recursive Lagrangian formulation of manipulator dynamics and a comparative study of dynamics formulation complexity, *IEEE Trans. Systems, Man, and Cybernetics*, 10(11), 730-736(1980).

[31] G. Rodriguez, Kalman filtering, smoothing and recursive robot arm forward and inverse dynamics, *IEEE Transaction on Robotics and Automation*, RA 3(6), 624-639(1987).

[32] R. Brockett, Finite dimensional linear systems, New York: John Wiley, 1970.

[33] A. Samuel, P. McAree, and K. Hunt, Unifying screw geometry and matrix transformations, *International Journal of Robotics Research*, 10(5), 454-472(1991).

[34] N. Bedrossian and M. Spong, Feedback linearization of robot manipulators and riemannian curvature, *Journal of Robotic Systems*, 12(8), 541-552(1995).

[35] F. Park, J. Bobrow, and S. Ploen, A lie group formulation of robot dynamics, *International Journal of Robotics Research*, 14(6), 609-618(1995).

[36] S. Ploen, *A lie group formulation of Lagrangian robot dynamics*, Thesis, University of California, Irvine, 1994.

[37] J. Selig, *Geometrical methods in robotics*, New York, Springer, 1996.

[38] I. Chen, and G. Yang, Automatic generation of dynamics for modular robots with hybrid geometry, *Proceedings of the IEEE International Conference on Robotics and Automation*, Albuquerque, NM, 2288-2293(1997).

[39] Y. Hwang, and N. Ahuja, Path planning using a potential field representation, *Proceedings of the IEEE International Conference on Robotics and Automation*, 24-29(1988).

[40] O. Khatib, Real-time obstacle avoidance for manipulators and mobile robots, *Proceedings of the IEEE International Conference on Robotics and Automation*, St. Louis, MO, 500 - 505(1985).

[41] W. Newman and N. Hogan, High speed robot control and obstacle avoidance using dynamic potential functions, *Proceedings of the IEEE International Conference on Robotics and Automation*, San Francisco, 14 - 24(1986).

[42] B. Favejon and P. Tournassoud, A local approach for path planning of manipulators with a high number of degrees of freedom," *Proceedings of the IEEE International Conference on Robotics and Automation*, 1152-1159(1987).

[43] F. Miyazaki and S. Arimoto, Sensory feedback based on the artificial potential for robots, in Proceedings of 9th IFAC (Budapest), 1984.

[44] V. Pavlov and A. Voronin, The method of potential functions for coding constraints of the external space in an intelligent mobile robot, *Soviet Automation Control*, 6, 1984.

[45] S. Suh and K. Shin, A variational dynamic programming approach to robot-path planning with a distance-safety criterion, *IEEE Journal of Robotics and Automation*, 4(3), 334-349(1988).

[46] S. Sastry, *Nonlinear Systems, Springer*, New York, 1999.

[47] H. Khalil, *Nonlinear systems*, 3rd ed., Prentice Hall, New *Jersey*, 2002.

[48] V. Utkin, J. Guldner, and J. Shi, *Sliding mode control in electro-mechanical systems*, 2nd ed., CRC Press, 2009.

[49] M. Zhihong, A. Paplinski, and H. Wu, A robust MIMO terminal sliding mode control scheme for rigid robotic manipulators, *IEEE Transaction on Automatic Control*, 39(12), 2464-2469(1994).

[50] A. Amer, E. Sallam, and W. Elawady, A new adaptive fuzzy sliding mode control using fuzzy self-tuning for 3 DOF planar robot manipulators, *Applied Intelligence*, 2(9), Online-first(2011)

[51] J. Slotine and W. Li, *Applied nonlinear control*, Prentice-Hall, Englewood Cliffs, N.J., 1991

[52] K. Astrom and H. Wittenmark, *Adaptive control*, Addison - Wesley, 1989.

[53] I. Kucukdemiral and G. Cansever, "Sugeno based robust adaptive fuzzy sliding mode controller for SISO nonlinear systems", *Journal of Intelligent & Fuzzy Systems*, 17(2), 113–124(2006).

[54] S. Tong and H. Li, Fuzzy adaptive sliding mode control for MIMO nonlinear systems, *IEEE Trans. on Fuzzy Systems*, 11(3), 354-360(2003).

[55] Y. Zhao, Y. Zhang, J. Yang, and L. Chen, Enhanced fuzzy sliding mode controller for robotic manipulators, *International Journal of Robotics and Automation*, 22(2), 170-183(2007).

[56] F. Behi, Kinematic analysis for a six-degree-of-freedom 3-PRPS parallel mechanism, *IEEE Journal of Robotics and Automation*, 4(5), 561–565(1988).

[57] J. Moren and C. Balkenius, A computational model of emotional learning in the amygdala, in J. A. Mayer, A. Berthoz, D. Floreano, H. L. Roitblat and S. W. Wilson (Ed.): From animals to Animals 6, *in Proc. of the 6th Int. Conf. on the Simulation of Adaptive Behaviour,* MIT Press, 383-391(2000).

[58] J. Moren, *Emotion and learning-a computational model of the amygdale*, Doctoral dissertation, Lund University, Sweden, 2002.

[59] O. Mowrer, *Learning theory and behavior*, Wiley, 1960.

[60] C. Lucas, D. Shahmirzadi, and N. Sheikholeslami, Introducing BELBIC: brain emotional learning based intelligent controller, *Intelligent Automation and Soft Computing*, 10(1), 11-21(2004).

[61] A. Mehrabian, and C. Lucas, Emotional learning based intelligent robust adaptive controller for stable uncertain nonlinear systems, *International Journal of Intelligent Technology*, 1, 246-252(2005).

[62] C. Kim and R. Langari, Mobile robot target tracking via a brain limbic system based control, *International Journal of Robotics and Automations*, 26(3), 11-21(2011).

[63] H. Yi and R. Langari, A design and bio-inspired control of a novel redundant manipulator with m-dof links, *International journal of Robotics and automation*, 27(4), 396-402(2012).

[64] O. Khatib, Motion and force control of robot manipulators, *Proceedings of the IEEE International Conference on Robotics and Automation*, 3, 1381–1386(1986).

[65] H. Seraji, Configuration control of redundant manipulators: theory and implementation, *IEEE Trans. on Robotics and Automat*ion, 5, 472-490(1989).

[66] B. Siciliano, Kinematic control of redundant robot manipulators: a tutorial, *Journal of Intelligent and Robotic Systems*, 3, 201–212(1990).

[67] M. Avriel, M. Rijckaert, and D. Wilde, *Optimization and Design*, Prentice-Hall, 1973.

[68] R. Malak, J. Aughenbaugh, and C. Paredis, Multi-attribute utility analysis in set-based conceptual design, *Computer-Aided Design*, 41, 214-227(2009).

[69] R. Marler and J. Arora, *Review of multi-objective optimization concepts and methods for engineering*, University of Iowa, Optimal design laboratory, Iowa City, IA (2003).

[70] R. Marler and J. Arora, Survey of multi-objective optimization methods for engineering, *Structure Multidisciplinary Optimization*, 26, 369–395(2004).

[71] P. Ferreira and M. Machado, Solving multiple-objective problems in the objective space, *Journal of Optimization Theory and Applications*, 89, 659-680(1996).

[72] J. Neumann and O. Morgenstern, *Theory of games and economic behavior*, Princeton, N. J. 1944.

[73] N. Metropolis and S. Ulam, The monte carlo method, *Journal of the American Statistical Association*, 44, 335–341(1949).

[74] T. Elperin, I weissberg, and E. zahavi, Machine design optimization by the monte carlo anneling method, *Engineering optimization*. 15, 193-203(1990).

[75] M. Yim, P. White, M. Park, and J. Sastra, Modular self-reconfigurable robots, *Encyclopedia of Complexity and Systems Science*, Springer, 5618-5631(2009).

[76] M. Yim, D. Duff, and K. Roufas, PolyBot: a modular reconfigurable robot, *Proceedings of the IEEE International Conference on Robotics and Automation*, San Francisco, CA, USA, 514 – 520(2000).

[77] S. Stramigioli and H. Bruyninckx, Geometry and screw theory for robotics, *Proceedings of the IEEE International Conference on Robotics and Automation*, Seoul, Korea, Tutorial 9 (2001).

[78] A. Karger and J. Nov´ak, *Space kinematics and lie groups*, New York: Gordon and Breach Science ublishers, 1985.

[79] R. Brockett, Robotic manipulators and the product of exponentials formula, *Mathematical Theory of Networks and Systems*, 58, 120-129 (1984).

[80] B. Siciliano, L Sciavicco, L. Villani and G. Oriolo, *The robotics: modeling, planning and control*, London: Springer, 2010.

[81] C. Chvallereau and W. Khalil, A new method for the solution of the inverse kinematics of redundant robots, *Proceedings of the IEEE International Conference on Robotics and Automation*, l, 37- 42(1988).

[82] E. Conkur and R. Buckingham, Clarifying the definition of redundancy as used in robotics, *Robotica*, 15, 583-586(1997).

[83] O. Egeland, Task-space tracking with redundant manipulators, *IEEE Journal of Robotics and Automation*, 3, 471-475(1987).

[84] J. Baillieul, Kinematic programming alternatives for redundant manipulators, *Proceedings of the IEEE International Conference on Robotics and Automation*, St. Louis, Missouri. 722-728(1985).

[85] J. Sagli, I. Spangelo, and O. Egeland, Resolving redundancy through a weighted damped least-squares solution, NTNU (Department of Engineering Cybernetics), 14(2), 107-119(1993).

[86] H. Seraji and R. Colbaugh, Improved configuration control for redundant robots, *Journal of Robotic Systems*, 7(6), 897-928(1990).

[87] B. Nobel and J. W. Daniel, *Applied linear algebra*, Englewood Cliff, Prentice-Hall, 1988.

[88] Y. Umetani and K. Yoshida, 2001, Workspace and manipulability analysis of space manipulator, *Transaction of the Society of Instrument and Control Engineers*, E, pp. 1-8.

[89] J. Lee, A study on the manipulability measure for robot manipulators, *Proceedings of the IEEE/RSJ International Conference on Intelligent Robotics and Systems*, 7-11, Grenoble, France, 1458-1465(1997).

[90] S. Ploen, *Geometric algorithms for the dynamics and control of multi-body systems*, Dissertation, University of California at Irvine, 1997.

[91] J. Latombe, *Robot motion planning*, Kluwer Academic Publishers: Boston, 1991.

[92] S. GE and Y. CUI, Dynamic motion planning for mobile robots using potential field method, *Autonomous Robots*, 13, 207–222(2002).

[93] J. Borenstein and Y. Koren, Real-time obstacle avoidance for fast mobile robots, *IEEE Transactions on System, Man, and Cybernetics*, 19, 1179- 1187(1989).

[94] A. B. Doyle and D. I. Jones, A tangent based method for robot path planning, *Proceedings of the IEEE International Conference on Robotics and Automation*, 2, 1561– 1566, 1994.

[95] S. Akishita, T. Hisanobu, and S. Kawamura**.,** Fast path planning available for moving obstacle avoidance by use of Laplace potential", *Proceedings of the 1993 IEEE/RSJ International Conference*, 1(1), 673 -678(1993).

[96] R. Arkin, *Behavior-Based Robotics*, MIT Press, Cambridge, Massachusetts, 1998

[97] R. A. Brooks, *Cambrian Intelligence: The Early History of the New AI*. MIT Press, Cambridge, Massachusetts, 1999.

[98] R. Murphy, *Introduction to AI Robotics*, MIT Press, 2000.

[99] I. Kucukdemiral, G. Cansever, Sugeno based robust adaptive fuzzy sliding mode controller for SISO nonlinear systems, *Journal of Intelligent & Fuzzy Systems*, 17, 113–124(2006).

[100] H. Yi, J. Yoo, and R. Langari, Dynamic analysis and sliding mode control of a novel extendable modular multi-DOFs link, *Proceeding of the ASME 2012 International Mechanic Engineering Congress and Exposition*, Houston, USA, 2012.

[101] P. Eric, O. Timothy, and S. Hayati, JPL serpentine robot: a 12 DOF system for inspection, *Proceedings of the IEEE International Conference on Robotics and Automation*, Nagoya, Japan, 3143-3148,1995.

APPENDIX

The aforementioned algorithm can derive the resulting equation of motion of the proposed manipulator as follows,

$$M(q)\ddot{q} + C(q, \dot{q})\dot{q} + \phi(q) = \tau$$

where

$$M(q) = \begin{bmatrix} m_{11}(q) & m_{12}(q) & m_{13}(q) & m_{14}(q) & m_{15}(q) & m_{16}(q) & m_{17}(q) \\ m_{21}(q) & m_{22}(q) & m_{23}(q) & m_{24}(q) & m_{25}(q) & m_{26}(q) & m_{27}(q) \\ m_{31}(q) & m_{32}(q) & m_{33}(q) & m_{34}(q) & m_{35}(q) & m_{36}(q) & m_{37}(q) \\ m_{41}(q) & m_{42}(q) & m_{43}(q) & m_{44}(q) & m_{45}(q) & m_{46}(q) & m_{47}(q) \\ m_{51}(q) & m_{52}(q) & m_{53}(q) & m_{54}(q) & m_{55}(q) & m_{56}(q) & m_{57}(q) \\ m_{61}(q) & m_{62}(q) & m_{63}(q) & m_{64}(q) & m_{65}(q) & m_{66}(q) & m_{67}(q) \\ m_{71}(q) & m_{72}(q) & m_{73}(q) & m_{74}(q) & m_{75}(q) & m_{76}(q) & m_{77}(q) \end{bmatrix},$$

$$C(q,\dot{q}) = \begin{bmatrix} c_{11}(q,\dot{q}) & c_{12}(q,\dot{q}) & c_{13}(q,\dot{q}) & c_{14}(q,\dot{q}) & c_{15}(q,\dot{q}) & c_{16}(q,\dot{q}) & c_{17}(q,\dot{q}) \\ c_{21}(q,\dot{q}) & c_{22}(q,\dot{q}) & c_{23}(q,\dot{q}) & c_{24}(q,\dot{q}) & c_{25}(q,\dot{q}) & c_{26}(q,\dot{q}) & c_{27}(q,\dot{q}) \\ c_{31}(q,\dot{q}) & c_{32}(q,\dot{q}) & c_{33}(q,\dot{q}) & c_{34}(q,\dot{q}) & c_{35}(q,\dot{q}) & c_{36}(q,\dot{q}) & c_{37}(q,\dot{q}) \\ c_{41}(q,\dot{q}) & c_{42}(q,\dot{q}) & c_{43}(q,\dot{q}) & c_{44}(q,\dot{q}) & c_{45}(q,\dot{q}) & c_{46}(q,\dot{q}) & c_{47}(q,\dot{q}) \\ c_{51}(q,\dot{q}) & c_{52}(q,\dot{q}) & c_{53}(q,\dot{q}) & c_{54}(q,\dot{q}) & c_{55}(q,\dot{q}) & c_{56}(q,\dot{q}) & c_{57}(q,\dot{q}) \\ c_{61}(q,\dot{q}) & c_{62}(q,\dot{q}) & c_{63}(q,\dot{q}) & c_{64}(q,\dot{q}) & c_{65}(q,\dot{q}) & c_{66}(q,\dot{q}) & c_{67}(q,\dot{q}) \\ c_{71}(q,\dot{q}) & c_{72}(q,\dot{q}) & c_{73}(q,\dot{q}) & c_{74}(q,\dot{q}) & c_{75}(q,\dot{q}) & c_{76}(q,\dot{q}) & c_{77}(q,\dot{q}) \end{bmatrix},$$

$$G(q) = \begin{bmatrix} gm_{11} & gm_{22} & gm_{33} & gm_{44} & gm_{55} & gm_{66} & gm_{77} \end{bmatrix}^T$$

$q_i = \theta_i$, ci=cosθ_i, si=sinθ_i, c_2θ_i = cos2θ_i, s_2θ_i = sin2θ_i,

Li= ith *Link length*, dtdqi = $\frac{d\theta_i}{dt}$, *Ixi* = the momentum of inertia of link i,

K0 = L3(m6+2m7)+L7m7c7,

K1 = K0c5s6+L7m7s5s7,

K2 = K0-L7m7c5s7,

K3 = c3s6+s3c5c6,

K4 = c3c6-s3c5s6,

K5 = L1+L2+L3+q4,

K6 = c5c7+s5s6s7,

K7 = s5c7-c5s6s7,

K8 = 8Ix7-8Iy7+2L3^{2}m6+8L3^{2}m7+L7^{2}m7,

K9 = 2L1+L2+2L3+2q4,

K10 = s5s7+c5s6c7,

K11 = s3s6-c3c5c6,

K19 = m4+m5+m6+m7,

K13 = 2L3K19+L2m5+2L2m6+2L2m7,

K12 = L1m4+2L1m5+2L1m6+2L1m7+K0c6+K13,

K14 = s3c6+c3c5s6,

K15 = 32Ix6+16Ix7-32Iy6-16Iy7-4L3^{2}m6-16L3^{2}m7+2L7^{2}m7+2K8c_2q6
+L7^{2}m7c_2q6c_2q6+8L3L7m7c_2q6c_2q6-16L3L7m7c7-6L7^{2}m7c_2q7,

K16 = dtdq2s3s5+dtdq3c5,

K17 = 4Ix7+L7^{2}m7+2L3L7m7c7,

K18 = L3+L7c7,

K20 = c5s7-s5s6c7,

K21 = s3c5(L1+L2+L3)+L3K3,

K22 = K8+8L3L7m7c7+L7L7m7c_2q7,

K23 = s3c5dtdq2-s5dtdq3,

K24 = s5c7+c5s6s7,

K25 = c5s7+s5s6c7,

K26 = dtdq1K4+dtdq4c6+S6K5K16,

K27 = dtdq2K3-dtdq3s5c6+dtdq5s6,

K28 = dtdq2K4+dtdq3s5s6+dtdq5c6,

K29 = dtdq2s3c5-dtdq3s5,

$M_{11}(q) =$ m1+m2+m3+K19,

$M_{12}(q) =$ 0,

$M_{13}(q) =$ 1/2((-L2(m5+2m6+2m7)-L3m3+L1m4-2(L1+L3+q4)K19)s3+K11K0-c3s5s7L7m7),

$M_{14}(q) =$ K19c3,

$M_{15}(q) =$ 1/2s3s5s6K2,

$M_{16}(q) =$ -1/2K0K3,

$M_{17}(q) =$ -1/2L7m7(s3s5c7+K4s7),

$M_{21}(q) =$ 0,

$M_{22}(q) =$ 1/4(4Iz2+4Ix3+4Iz5c3c3+(4Ix5+L3L3m3+4(m5+m6))K5K5s3s3+4Ix6K4K4+4Iy7(c3c6c7-s3K10)(c3c6c7-s3K10)+2m4K5K5+s3s3s5s5[2m6(c3s6+c6)K5L3+m6L3L3+4Iy6]+K3(2s3c5L3m6K5+s3c5(c6+c3s6)(4Ix6+L3L3m6)+2m7s3s5(L3+K5c6)L7((s3s5c7c7+(L3+K5c6)(1+2s3s5))+s7K4)+(s3s5c7+K4s7)(4Iy7+L7L7m7)(K7+c3c6s7)s3)+4m7(K5s3s5s6c7-21s7)k21s7+2m7(s3K5K6+K3L3c7)(2+K3L7)+K3(2L7m7K5(4Ix7+L7L7m7+2L3L7m7c7))),

$M_{23}(q) =$ 1/16((L1+4L2+4L3c7)L3m6s3s_2q5s6s6-8K5K0c3s5s6-16(Ix7-4Iy7)K3s5c6-2L3s5s6(L3m6+4L3m7+4L7m7c7)(K4+c3c6)-4L7m7s6(s5c7(c3c6c7-s3s5s7)+2s3c5c5s7L3(L3+c7))+L7m7c5(-L7s3s5(c6c6-3(2c7c7-1)+(2c6c6-1)(2c6c6-1))+4c3s7(2K5+c6(2L3+L7c7)))),

$M_{24}(q) =$ -1/2s3s5s6K2

$M_{25}(q) =$ 1/16(c3(16Ix6+16Iy7+16Iz5+K8(1-c_2q6)-L7m7(8L3+3L7)c_2q6c_2q6+L7m7(8L3c7-L7c_2q7))+s3(2c5s6(c6(K8+8L3L7m7c7+L7L7m7c_2q7)+4K5K0)+4L7m7s5s7(2K5+c6(2L3+L7c7))))

$M_{26}(q) =$ 1/4(L7m7s7(2L3+L7c7)K4+s3s5(4Iy6+4Iy7+L3(L3m6+4L3m7+4L7m7c7)+2K5K0c6-L7L7m7s7s7)),

$M_{27}(q) =$ -1/2(2Ix7+L7L7m7+L3L7m7c7)K3-1/2L7m7s3K5K6,

$M_{31}(q) =$ 1/2((-L2(m5+2m6+2m7)-L3m3+L1m4-2(L1+L3+q4)K19)s3+K11K0-c3s5s7L7m7),

$M_{32}(q) =$ 1/16((L1+4L2+4L3c7)L3m6s3s_2q5s6s6-8K5K0c3s5s6-16(Ix7-4Iy7)K3s5c6-2L3s5s6(L3m6+4L3m7+4L7m7c7)(K4+c3c6)-4L7m7s6(

s5c7(c3c6c7-s3s5s7)+2s3c5c5s7L3(L3+c7))+L7m7c5(-L7s3s5(c6c6-3(2c7c7-1)+(2c6c6-1)(2c6c6-1))+4c3s7(2K5+c6(2L3+L7c7)))),

$M_{33}(q) =$ 1/4(4Iy3+4Ix5+L3L3m3+L1L1m4+4Ix6s5s5s6s6+4Iy7(K7K7+K6K6)+c5c5((4Ix6+L3^{2}m6)s5^2+4Iy6+m6L3L3)+2m4(L3+q4)(2L1+2L3+2q4)+2m5K5K9+4m6K5(K5+L3L3c6)+4m7c5(L3+K5c6)(K6L7+(L3+K5c6)c5)+4m7(K5K10+L3s5c6s7)(K5K10+L3s5c6s7)+2m7(K5K7+L3s5c6c7)(s5c6L7+K5K7+L3s5c6c7)+s5c6(s5c6K17+2m7K5K7L7)+L7L7m7K6K6),

$M_{34}(q) =$ -1/2(c5s6K0+s5s7L7m7),

$M_{35}(q) =$ -1/4((2K5K0+c6K22)s5s6-L7m7c5s7(2K5+c6(2L3+L7c7))),

$M_{36}(q) =$ 1/4(c5(4Iy6+4Iy7+L3L3m6+L7L7m7c7c7+4L3m7(L3+L7c7)+2c6K5K0)+L7m7(2L3+L7c7)ss6s7),

$M_{37}(q) =$ (Ix7+L7L7m7/4)s5c6+1/2L7m7(K5K7+L3s5c6c7),

$M_{41}(q) =$ K19c3,

$M_{42}(q) =$ -1/2s3s5s6K2,

$M_{43}(q) =$ -1/2(c5s6K0+s5s7L7m7),

$M_{44}(q) =$ m4+m5+m6+m7,

$M_{45}(q) =$ 0,

$M_{46}(q) =$ -1/2K0s6,

$M_{47}(q) =$ -1/2L7m7c6s7,

$M_{51}(q) =$ 1/2s3s5s6K2

$M_{52}(q) =$ 1/16(c3(16Ix6+16Iy7+16Iz5+K8(1-c_2q6)-L7m7(8L3+3L7)c_2q6c_2q6+L7m7(8L3c7-c_2q7L7))+s3(2c5s6(c6(K8+8L3L7m7c7+L7L7m7c_2q7)+4K5K0)+4L7m7s5s7(2K5+c6(2L3+L7c7)))),

$M_{53}(q) =$ -1/4((2K5K0+c6K22)s5s6-L7m7c5s7(2K5+c6(2L3+L7c7))),

$M_{54}(q) =$ 0,

$M_{55}(q) =$ Iz5+Ix6+Iy7-1/4c6c6s7s7L7L7m7+(L3L3m6/4+L7L7m7/4+L3L3m7+L3L7m7c7)s6s6,

$M_{56}(q) =$ 1/4L7m7c6s7(2L3+L7c7),

$M_{57}(q) =$ -1/4(4Ix7+L7L7m7+2L3L7m7c7)s6,

$M_{61}(q) =$ -1/2K0K3,

$M_{62}(q) =$ 1/4(L7m7s7(2L3+L7c7)K4+s3s5(4Iy6+4Iy7+L3(L3m6+4L3m7+4L7m7c7)
+2K5K0c6-L7L7m7s7s7)),

$M_{63}(q) =$ 1/4(c5(4Iy6+4Iy7+L3L3m6+L7L7m7c7c7+4L3m7(L3+L7c7)+2c6K5K0)+L7
m7(2L3+L7c7)s5s6s7),

$M_{64}(q) =$ -1/2K0s6,

$M_{65}(q) =$ 1/4L7m7c6s7(2L3+L7c7),

$M_{66}(q) =$ Iy6+Iy7+L3L3m6/4+L3^{2}m7+L7L7m7/8+L3L7m7c7+1/8L7L7m7c_2q7,

$M_{67}(q) =$ 0,

$M_{71}(q) =$ -1/2L7m7(s3s5c7+K4s7),

$M_{72}(q) =$ -1/2(2Ix7+L7L7m7+L3L7m7c7)K3-1/2L7m7s3K5K6,

$M_{73}(q) =$ (Ix7+L7L7m7/4)s5c6+1/2L7m7(K5K7+L3s5c6c7),

$M_{74}(q) =$ -1/2L7m7c6s7,

$M_{75}(q) =$ -(1/4)(4Ix7+L7L7m7+2L3L7m7c7)s6,

$M_{76}(q) =$ 0,

$M_{77}(q) =$ Ix7+L7L7m7/4,

$C_{11}(q,\dot{q}) =$ 0,

$C_{12}(q,\dot{q}) =$ 0,

$C_{13}(q,\dot{q}) =$ 1/2(-dtdq42s3K19+dtdq5c3(K0s5s6-L7m7c5s7)+dtdq6K0K11+dtdq7L7
m7(-2c3s5c7+s7K14)-dtdq3(c3(L1m4+L2m5+L3m3+2L1(m5+m6+m7
+2L2(m6+m7)+c6K0)+(4L1L3c3+2c3q4)K19)-s3(c5s6K0+s5s7L7m7))),

$C_{14}(q,\dot{q}) =$ -K19dtd3s3,

$C_{15}(q,\dot{q}) =$ 1/2(dtdq6s3s5c6K0-dtdq7L7m7s3s7K6+dtdq5s3(c5s6K0+L7m7s5s7)
+dtdq3c3(s5s6K0L7m7c5s7)),

$C_{16}(q,\dot{q}) =$ 1/2(K0(dtdq5s3s5c6+dtdq3K11-dtdq6K4)+L7m7dtdq7K3s7),

$C_{17}(q,\dot{q}) =$ 1/2L7m7(dtdq3(-c3s5c7+s7K12)-dtdq5s3K10+dtdq6s7K3-dtdq7(c3c6c7-s3K10)),

$C_{21}(q,\dot{q}) =$ 0,

$C_{22}(q,\dot{q}) =$ 1/128(-(64dtdq4c3^2+2dtdq3s_2q3)(K13+L1(m4+2(m5+m6+m7))+c6K0)
-64dtdq4(K12-K1s_2q3+(K12-L7m7c6c7-4q4K19)s3s3)+dtdq3(16c_2q3(
2(L1+L2+L3+4q4)(K0c5s6+4L7m7s5s7)+2(K8+L7L7m7c_2q7+4L3L7m7c7
)c5s6c6+4L7m7(2L3+L7c7)s5c6s7)+128K19s_2q3q4q4+s_2q3(-64Ix6
+64Iy6+128Ix5-28Iz5+128(L1^2+L1L2+L1L3)(m5+m6+m7)+32(L3L3m3
+L2L2m5+L3L7m7c7)+32(L1L1+4L1L3+4L3L3)m4+128(L1L3+L2L3+L3L3)
(m5+m6+m7+3c6m6)+12L7L7m7c_2q7+128(L2^2+L1L2+L2L3)(m6+m7)-
4(8Ix7-8Iy7-2L3^{2}m6-4L3^{2}m7+L7^{2}m7)+4(16Ix6-16Iy6+8Ix7-8Iy7-2L3^{2}m6
-L3^{2}m7+L7^{2}m7)c_2q5+2(K8+L7^{2}m7-40L3L7m7)c_2q5c_2q5+12(K8
+12(L7^{2}m7+8L3L7m7)c_2q6)c_2q6+(L7^{2}m7+8L3L7m7)(Cos[2q5-2q6-q7]
+Cos[2q6+q7])+128(L1+L2+L3)L7m7c6c6))+4dtdq6(-32L3(L1+L2
+L3)K0s3s3+4s_2q3[c5(K8c_2q6+4(L1+L2+L3)c6K+L7m7c_2q5(8L3c7
+L7c_2q7))-4L3L7m7s5s6s7)+2(K8+24L3L7m7c7)s_2q6c_2q3
+L7L7m7s_2q6((1+3c_2q3)(c7^2-s7^2))-2K8s3s3s_2q6c_2q5-
4L7m7s_2q5s_2q7(L7(s5s6+s3s3)+L3(2s3s3c6+s5s6))-2K0s3K11q4)
-4dtdq5(4s_2q3((4K5K0+c6K22)s5s6-2L7m7c5s7(2(K5+L3c3)+L7c6c7))
+s3s3((32Ix6-32Iy6+16Ix7-16Iy7-4L3^{2}m6-16L3^{2}m7+2L7^{2}m7+2K8c_2q6-
16L3L7m7c7+2L7(L7+8L3)m7c_2q6c_2q6-6L7^{2}m7c_2q7)s_2q5
+16L7m7(2L3+L7c7)s6s7c_2q5))+4L7m7dtdq7(16K7s_2q3q4+8L3s6^{2}s7
-16L3s3^{2}s6c7s_2q5-8L7s3^{2}s3^{2}s6^{2}s_2q7-16L3(1+c3^{2}s6^2)
+4L3^2(1+2c6^2)s7s_2q3+8L7(s5c6-c5s6c6)s_2q3s_2q7
+8L3^{2}s3^2(s7s3^{2}c_2q5-s6s_2q5)-32K5s3^{2}c6s7-16(L1+L2+L3
+2c6)c5s6s7s_2q3c_2q5-L7s_2q7(2s3^2)c_2q5(3c5^2-c6^2+c5^{2}s6^2))),

$C_{23}(q,\dot{q}) =$ -((Ix6+Iy6)dtdq3c5-4(Ix7+Iy7)(dtdq32c5c6^2+dtdq6c_2q6)c6^2)c3s5
+1/16(2(4Ix7+4Iy7+2L3L3m6+(8L3L3+L3L7c7+L7L7c7c7)m7)+s5(c3

dtdq6c_2q6s3s_2q6(dtdq3+2c5dtdq6))+8K5(K0s5(dtdq3s3s6-dtdq6c3 c6)-8L7m7s3c5s7dtdq3)+L7L7m7 c3s5dtdq3c5(6-1616s6s6c7-c6c6c7c7) +dtdq3c3s5c5s6s6(9L7L7m7+4L3L3m6)-8c3dtdq4(K0s5s6+L7m7c5s7) -8L3L7m7(dtdq3c5+dtdq6c5^2-s5^2)(c6+s6)s3s7 +1/2L7L7m7c3s_2q5(dtdq3(1+2c7c7)s6s6+1/2dtdq3c6c6s7s7s_2q5-dtdq3s7s7)-L7L7m7s3s5s7s7((dtdq3+2c5dtdq6)s_2q6-dtdq6c_2q6c6c6) -2dtdq3L7L7 m7 s_2q7c5(1+c5)(s3c6+c3s6)-1/2dtdq5(c5(s3c5K15 +4c3s6(4K5K0+c6K22))+(8L7m7c3s5s7(2(K5+L3c6)+c6L7c7)-s3(s5s5K15 +16L7m7s_2q5s6s7(2L3+L7c7))))+4L7m7dtdq7(c3(2(K6)(K5+L3c6) +2s6c6s5s7(L3+L7c7)+L7c5c6c_2q7)-s3(L7s6(c_2q5c_2q7)-L3s5s5s6c7-2L3s5(c7(s5s6-2c5s7)+c5s7(c6c6c7-2s6s6s7))))),

$C_{24}(q,\dot{q}) =$ 1/2(-K0(dtdq6s3s5c6+dtdq5s3c5s6+dtdq3c3s5s6)+L7m7(dtdq3c3c5s7-dtdq5s3s5s7+dtdq7s3K6)),

$C_{25}(q,\dot{q}) =$ 1/32(2dtdq3(s3(-16Ix6-8Ix7-8Iy7-16Iz5-2L3L3(m6+4m7)+K8c_2q6 +L7L7m7(c_2q7-3+c_2q6c_2q6)-L3L7m7(c7+c_2q6c_2q6)) +c3(8K0K5c5s6+8L7m7s5s7(K5+L3c6)+2L7L7m7s5c6c_2q7+K8c5s_2q6 +L7m7c5s_2q6(8L3c7+4L3c7+s_2q6c_2q7c5)))+4dtdq6(s3c5(K8c_2q6+ 4K5c6K0+L7m7(8L3c7+L7c_2q7)c_2q6)+K8c3s_2q6+(8L3L7c7-L7L7c_2q7)m7c3s_2q6-(2L3+L7c7)L7m7s3s5s6s7)+4L7m7dtdq7(4(K5 +L3c6)s3s5c7-8L3c3s7s6s6-4(K5+2L3c6)s3c5s6s7-L7s3c5s_2q7s_2q6 +2L7s3s5c6c7^{2}c_2q7+2L7c3s6s6s_2q7)-2s3(-8dtdq4(c5s6K0+L7m7s5s7) +2dtdq5((4K5K0+c6K22)s5s6-4L7m7c5s7(2(L1+L2+L3+L3c6)+c6L7c7)))),

$C_{26}(q,\dot{q}) =$ 1/8((8Iy6+8Iy7+*2L3^{2}m6+8L3^{2}m7*+L7^{2}m7)c3s5dtdq3+4K5K0s5(dtdq3c3c 6-tdq6s3s6)+L7m7dtdq3c3s5(c78L3+c_2q7L7)-2L7m7((dtdq3 +dtdq6)K11-tdq7K4)(2L3s7+L7c7)+dtdq4K0s3s5c6+dtdq5s3(c5(8Iy6 +8Iy7+2L3L3m6+8L3L3m7+L7L7m7+8L3L7m7c7+4K0K5c6+L7L7m7c_2q 7)+2L78m7(2L3+L7c7)s5s6s7-2s5s7(2L3+K5c6+L7c7))),

$C_{27}(q,\dot{q}) =$ 1/4(dtdq5((4Ix7+L7^{2}m7)s3s5c6+2L3L7m7(s5c7+K6s7))+2L7m7(s5c6s7dt dq6((L1+L2+L3)s3s3+q4c5)+c3dtdq3K5(s3s5s6s7-c5c7)+s3K5(K7dtdq5 +K20dtdq7)-dtdq4s3K6)+(4Ix7+L7L7m7+2L3L7m7c7)(K4dtdq6-

K11dtdq3)),

$C_{31}(q,\dot{q}) =$ 1/2(-2K19dtdq4s3-7m7dtdq7(c3s5c7+K11)+K0dtdq6K11
+((L3m6+2L3m7)s5s6+L7m7dtdq2K20)(dtdq2+c3dtdq5)-
dtdq3(c3(K13+L3m3)-s3(c5s6K0+L7m7s5s7)+2M14q4)),

$C_{32}(q,\dot{q}) =$ 1/32(2L7m7dtdq7(4c3(2(K5+c6(2L3+L7c7))s5s6s7+2(L1+L2+L3+L4+L3c6
)c5c7+L7c5c6(c7c7s7s7+c_2q7))-2s3(2c5c5s6(2L3c7
+L7c_2q7)c_2q5+(4L3s6s6s7-L7s_2q7(1+s6s6))s_2q5
+2L7s5s5s6s7s7))-dtdq2(4c_2q3((4K5K0+c6K22)c5s6+2L7m7(2K5
+c6(2L3+L7c7))s5s7)+16s_2q3(K12+K19q4)+1/8s_2q3(128Ix5-128Iz5-
2(64Ix6-64Iy6-K8)s5s5+32(L3L3m3+L1L1m4+L2L2m5+(4L1+4L3)(L3m4
+L2m5))+16L3L3(m6+4m7)+64((L1+L2)(L1+L2)+(L2+L3)(L2+L3)+(L1+L3)(
L1+L3))(m6+m7)+128(L1+L2+L3)(2m5+m6c6+2m7c6)L3-
16(m6+4m7)L3L3c_2q5+32L3L7m7c7+4K8c_2q6(c_2q6+2)
+16L3L7m7(c_2q5c_2q6+s_2q5s_2q6-2)c_2q5c_2q5+128L7m7(L1
+L2+2L3)c_2q6c_2q6+2L7^{2}m7((c5c6-s5s6)(c5c6-s5s6)+(c5c6
+s5s6)(c5c6+s5s6)-(c_2q5c_2q5-c_2q6c_2q6))+4L7m7(3L7c_2q7
+2(8L3+L7)s6s6))))+2L7L7m7(1+c6c6)c3dtdq3(1-7c7)c5s5-
16L7m7s3c5s7q4dtdq3+4s5dtdq6(4K0s3s6q4-4K0K0c3c6-K8c3c6c6)-
L7m7c3s5c7(-L7c5c7dtdq3+c6c6(4dtdq6L3+L7c7dtdq6))-
4L7L7m7c3s5s7s7(dtdq3(1+s6s6)c5-tdq6c_2q5c6c6)-(K8(1+c6c6)
+16(Ix6-Iy6-L3L7m7s6s6c7))c3dtdq3s_2q5-L7L7m7s7s7s3
s_2q6(s5dtdq3+2c5dtdq6)-4L7L7m7dtdq3s_2q7(c5+c_2q5)(s3c6
+c3s6)-dtdq5(4c3c5s6(4K5K0+c6K22)+8L7m7c3s5s7(2K5+c6(2L3
+L7c7))-((32Ix6-32Iy6+4K8s6s6+L7m7(L7c_2q6c_2q6+8L3c_2q6c_2q6
-16L3c7-L7c_2q7))(s3s5s5+2s3c5c5)+16L7m7(2L3
+L7c7)s3s6s7s_2q5)),

$C_{33}(q,\dot{q}) =$ 1/16(-L7m7c3s5c5s6s6dtdq2(L7+L7c7c7+2L3c7)+(8Ix6-8Iy6)(dtdq2c3
+dtdq5)s_2q5+(4Ix7-4Iy7-L3L3m6-4L3L3m7)s_2q5((1+c6c6)dtdq5
+2dtdq2c3)-K8s_2q6(dtdq2s3s5+dtdq5s6s6+2dtdq6s5s5)+8L7m7(L3c3

s6s7c_2q5+(L1+L2+L3+L4+L3c6)s3c5s7)dtdq2-8K0(L3m6+q4)s3s5
s6dtdq2+L7^{2}m7dtdq2(s3s5s_2q6s7^2+2s_2q7(K3(c5^2-s5^2))+c3s5c5(2s7^2
+2s6^{2}s7^2-s6^2-s6^{2}c7^2))+L7m7(-8L3c7s6^{2}s_2q5(-8L3c7s6^2-L7c7^2(s6^2
+2c7^2)+L7s7^2(2+2s6^2))+8L7m7s6s7(L7c7+2L3)(c5^2-s5^2))dtdq5+(2L7m7(
L7s_2q7s_2q5c6-L7s_2q6s7^{2}s5^2+4L3c6s7s_2q5)-16K0(L3m6
+q4)s6)dtdq6+L7m7(4L3s5^{2}s7(3s6^2-c6^2)-(-2c5^2+3s5^2-s5^{2}c6^2-2s5^{2}s6^{2}s5^2)
L7s_2q7-(12L3+4L3c5c5+16K5c6)s7+4((2L3+L7c7)c7-7s7^2)s_2qs6)dtdq7
+16dtdq4(K12+2K19q4)+8dtdq1(c3K12-(c5s6K0+L7m7s5s7)+2M14q4)),

$C_{34}(q,\dot{q}) =$ 1/2(-c5c6K0dtdq6+2K19dtdq1s3+(K0s5s6-L7m7c5s7)(dtdq2c3+dtdq5)-
L7m7dtdq7K7),

$C_{35}(q,\dot{q}) =$ 1/16(dtdq2((16Ix6+16Iy7+16Iz5+K22-K8c_2q6-L7L7m7c_2q6c_2q6
+8L3L7m7c7+4L7L7m7s7s7)s3c_2q6-2c3(c5s6(4K5K0+c6K22)
+L7m7s5s7(4(K5+L3c6)+2L7c7c6)))+4L7m7dtdq7(2(K5+c6(2L3+L7c7))s5
s6s7+c5(2(K5+L3c6)c7+L7c6c_2q7))-2((K8-L7L7m7)c5s_2q6dtdq5
+4K5(K0c5s6+L7m7s5s7)dtdq5+2L7m7 c6dtdq5 (L7s7K10
+2L3(K10+c5s6c7))+4(K0s5s6-L7m7c5s7)(dtdq1c3+dtdq4)
+dtdq6(4s5c6K5K0+s5K22c_2q6+(2L7m7c5(2L3+L7c7)s6s7)))),

$C_{36}(q,\dot{q}) =$ 1/8(4c5c6K0dtdq4-((8Iy6+8Iy7+2L3L3m6+8L3L3m7+L7L7m7+4K5K0
+8L3L7m7c7+L7L7m7c7c7dtdq2)s5-(4L3L7+L7L7
+2L7L7c7)m7c5s6s7)(dtdq2c3+dtdq5)-4K5c5(K0s6dtdq6+
L7m7c6s7dtdq7)-4K0dtdq1K11+2L7m7dtdq7(2L3K20(2L3
+L7c7)-L7s5s6s7s7)+(4L3L7+L7L7)m7c6s7(s3dtdq2+s5dtdq6)),

$C_{37}(q,\dot{q}) =$ ((Ix7+L7^{2}m7/4)K6-1/2L7m7c5(L3+K5c6))(dtdq2(s3s5s7-K4c7)
+dtdq3K20+dtdq6s7-dtdq5c6c7)-1/2L7m7(dtdq7-dtdq2K3+dtdq3s5c6-
dtdq5s6)((L1+L2+L3+q4)K10+L3s5c6s7)-1/2L7m7c6s5(L3K27s7-
c7(dtdq1K4+dtdq4c6)+s3s7s5dtdq1+K7s3dtdq2K5-K10dtdq3K5)-K20(-
(Ix7s7+L7L7m7s7/4)(c6(dtdq2c3+dtdq5)+(dtdq3s5-dtdq2s3c5)s6)
+1/2L7m7((dtdq1c3+dtdq4)s6-c6(dtdq3c5K5-s3(c5dtdq1
-dtdq2s5K5)))-(c7(Ix7+L7L7m7/4)+1/2L3L7m7)(K16+dtdq6)),

$C_{41}(q,\dot{q}) =$ 0,

$C_{42}(q,\dot{q}) =$ 1/4(-2s3(K0(s5c6dtdq6+dtdq5c5s6)+s5s7L7m7)-L7m7dtdq7K6)
+dtdq2(-K12+c_2q5(K13+L1(K19+m5+m6+m7)+c6K0)-(K0c5s6
+L7m7s5s7)s_2q3-K19s3s3q4),

$C_{43}(q,\dot{q}) =$ -1/2(K0dtdq6c5c6-(K0s5s6-L7m7c5s7)dtdq5+L7m7dtdq7K7
+dtdq3(K12+2K19q4)),

$C_{44}(q,\dot{q}) =$ 0,

$C_{45}(q,\dot{q}) =$ 1/2(dtdq3(K0s5s6-L7m7c5s7)-dtdq2s3(c5s6K0+L7m7s5s7)),

$C_{46}(q,\dot{q}) =$ 1/2(-K0c6(K16+dtdq6)+L7m7dtdq7s6s7),

$C_{47}(q,\dot{q}) =$ 1/2L78m7(-c6c7dtdq7-K7dtdq3+dtdq6s6s7+dtdq2s3K6),

$C_{51}(q,\dot{q}) =$ 1/4(2s3(c6K0dtdq6s5+dtdq5(K0c5s6+s5s7L7m7)-L7m7dtdq7K6)
+dtdq2(c3c3L2m5+(2(L1+L2+L3)(m5+m6+m7)+2(L1+L2+L3+q4)(m6+m7
)+2K0c6+K0c5s6+L7m7s5s7+L2m5+2L3m5+4m5q4)s3s3),

$C_{52}(q,\dot{q}) =$ 1/16(-16dtdq3(s3Iz5+Ix6c6K11)+K22c3dtdq6s_2q6-16K4Ix6s6(K16
+dtdq6)+4K4L7L7m7c6s7c7dtdq7-16Iy7(c6c7dtdq3(s3c6c7+2c3K10)-
s3K10K10dtdq3)+16Iy7(s6c7dtdq6-dtdq2s3K20+c6s7dtdq7)(s3K10-
c3c6c7)+8dtdq4s3(c5s6K0+L7m7s5s7)-2dtdq5s3((4K5K0+c6K22)s5s6-
2L7m7c5s7(2(K5+L3c6)+L7c6c7))+4dtdq3s6(2L3c3c5K5m6-
(4Ix6+L3L3m6+4Ix7)K11)+(L3m7c7+2L7)(-(L7+2L3c7)K11
+2c3K5K6)+4dtdq3c6s7(c3(L7(L7+2L3c7)s5-4Iy7+L7^{2}m7) 3K10c6s7))
+8s3c5K5(-2m6s3c5dtdq1+2(K5+L3c6)m6s3s5dtdq2+L3m6c6dtdq6-
L7m7s6s7dtdq7+2m6c5c6dtdq3K5L3)+4K3((4Ix6+L3^{2}m6)c6dtdq6-
2L3m6s3c5dtdq1-2L3L7m7s6s7dtdq7+(s3s5dtdq2+c5dtdq3)(2L3m6K5
+(4Ix6+L3^{2}m6)c6))-8m7s3s5(L3+K5c6)(2s3s5c6dtdq1-L7c6c7dtdq7-
L7s6s7dtdq6(tdq3s5-tdq2s3)(c5(2L3+2K5c6+L7c7)+L7s5s6s7))-
4(s3s5c7+K4s7)((4Iy7+L7^{2}m7)(s6s7dtdq6-c6c7dtdq7)+dtdq3(-
s5(2L3L7m7+2K5L7m7c6+(4Iy7+L7^{2}m7)c7)+(4Iy7+L7^{2}m7)c5s6s7)+2L7m
7dtdq1s3s5c6+dtdq2s3(c5(2L3L7m7+2K5L7m7c6+(4Iy7+L7^{2}m7)c7)+(4Iy
7+L7^{2}m7)s5s6s7))-16L3m7dtdq3s6s7(L3s3s6s7-3(K5K20+L3c6c5s7))
+16m7(K5s3s5(c6s7+s6c7)-L3K3s7)(-L3(s6c7+c6s7)dtdq7+(s3dtdq1

-K5dtdq3)K20-L3dtdq3c5c6s7-dtdq2s3(K5K10+L3s5c6s7))+8m7((K5
+L3c6)s3c5c7+s6(L3c3c7+K5s3s5s7))(c6(L7+2L3c7)dtdq6-
2dtdq1s3s5s6s7-c5c7dtdq1s3-2L3s6s7dtdq7+dtdq2L7s3s5c6
+dtdq2s3(s5(2(K5+L3c6)c7+L7c6)-
2K5c5s6s7)+dtdq3(c5(2(K5+L3c6)c7+c6L7)+2K5s5s6s7))+4K3((c5c6dtdq
3+c6dtdq6)K17-2L7m7dtdq1s3K6+s3dtdq2(2(K5+L3c6)L7m7K7
+4Ix7+L7L7m7s5c6)+dtdq3(2K5L7m7K6))-m5s3(L1+L3+q4)((s3s5dtdq2
-5dtdq3)c5K9+s5(2dtdq1(s3s5+c5c5)-(s5c5dtdq2+s5dtdq3)K9))-
c5s3(dtdq6(16+c6^2(8Iy7-L7^{2}m7c_2q7)+(8Ix7+2L3^{2}m6+8L3^{2}m7
+4L3L7m7c7+L7^{2}m7)s6^2)-2K16(4Ix5+L2m5(L1+L3+K5))
+4s3L2m5c5dtdq1)-8m6s3s5c6K5(2K23(L3+4K5c6)+4s3s5c6dtdq1)
-2s3s5(2K23(4Iy6+L3^{2}m6+4)+(8Iy7+L7^{2}m7-L7^{2}m7c_2q7)c6dtdq7
+4s3s5c6L3m6dtdq1)+8s3s5(-2m5(K23(L1+L3+q4)+s3s5dtdq1)(Ix5
+L2^{2}m5/4))-8s3s5s6^{2}K5(-7(2L3+L7c7)dtdq7+2m6(s3s5dtdq1+K23K5))),

$C_{53}(q,\dot{q}) =$ 1/128(16L7m7dtdq7(4c6((L3+L7c7)s5s6s7+L7c5c_2q7)+4(K5+L3c6)K6)-
dtdq2s3(128Ix5+64Ix6+32Ix7+64Iy6+96Iy7-128L1L2m5-96L2^{2}m5-
128L2L3m5+24L3^{2}m6+97L3^{2}m7+128(2L1(L2+L3)+2L2L3+L1^2+L2^2+L3^2+2(
L1+L3+q4)q4)(m5+m6+m7)+20L7^{2}m7-4(16Ix6-16Iy6+K8)c_2q5-(c_2q6
+c_2q5c6)+128K5L3c6(m6+2m7)+4L7m7c7(3c_2q5-4(3+L3)(c_2q5
c_2q6-_2q5s_2q6)+4L3(6+2c_2q5+c_2q6)+32(L1+L2+L3)c_2q6)
-2L7L7m7((c_2q5c_2q6)c_2q7+16s_2q5s6s7(2+c7))+128(L2m5
+2L2m6+2L2m7+c6L7m7c7)q4)-dtdq3((32Ix6-32Iy6+2K8+2K8c_2q6
+2L7m7((L7+8L3)c_2q6c_2q7-(8L3c7+3L7c_2q7)))s_2q5-32L7m7
c_2q5s6s7(2L3+L7c7))-8dtdq6(8K5c6K0s5+2s5c6c6K22-2s6(K22s5s6
-2L7m7c5s7(2L3+L7c7)))-(8dtdq4(s5s6K2)+dtdq5(2c5s6(4K5K0+c6(
L7L7m7c_2q7+K8+8L3L7m7c7))+48L7m7s5s7(2K5+c6(2L3+L7c7)))),

$C_{54}(q,\dot{q}) =$ 1/2(-dtdq3(K0s5s6-L7m7c5s7)+dtdq2s3(K0c5s6+L7m7s5s7)),

$C_{55}(q,\dot{q}) =$ 1/8(-4dtdq1s3(c5s6K0+L7m7s5s7)+(4K5(s5s6K0-c5s7L7m7)-
2L7^{2}m7c6c7K20+(K8-L7^{2}m7+4L3L7m7c7)s5s_2q6)dtdq2s3
+(K0+8L3L7m7c7+L7^{2}m7c_2q7)dtdq6s_2q6+4L3L7m7s7(-

L3+L3c6^2+L7c6^{2}c7)dtdq7+dtdq3((4K5K0+c6K22)c5s6
+2L7m7(2(K5+L3c3)+L7c6c7)s5s7)),

$C_{56}(q,\dot{q}) =$ 1/4L7m7c6((2L3c7+L7c_2q7)dtdq7-4K0s3s5c6dtdq1+(8Iy6+8Iy7
+2L3^{2}m6+8L3^{2}m7+L7^{2}m7+8L3L7m7c7+4K5K0c6+L7^{2}m7c7^2)(-
dtdq2s3c5+dtdq3s5)-L7m7s7((2c5s6L3+K10L7)dtdq3+s6dtdq6(2L3+c7)
-(2L3+L7c7)s5s6)),

$C_{57}(q,\dot{q}) =$ 1/4(-K17c6(dtdq6+s3s5dtdq2+dtdq3c5)+2L7m7s3K6dtdq1+2L3L7m7
s6s7dtdq7-2K5L7m7s3K7dtdq2-2dtdq3(L1+L2+L3+q4)L7m7K6),

$C_{61}(q,\dot{q}) =$ 1/8(-8(m6+m7)dtdq4s3c5-K04dtdq6K4-7m7dtdq2s7(3+(1+2s3^2)c_2q5)
+4L7m7s7(dtdq7K3-dtdq5c3)-8(K5(m6+m7)+c6K0)dtdq2(s3s5
+c5)c3+2K0s3c3s5c5s6dtdq2+2dtdq3(2s3c5c5K0s6+L7m7s3s_2q5s7)),

$C_{62}(q,\dot{q}) =$ 1/8(-(Ix6+L3^{2}m6/4)K5K28+K4((8Iy7+4L3L7m7c7
+L7^{2}m7L7^{2}m7c_2q7)dtdq7+8Ix6K27)-2L7m7dtdq6s7(2L3
+L7c7)K11+dtdq5s3(c5(8Iy6+8Iy7+2L3^{2}m6+8L3^{2}m7+L7^{2}m7
+8L3L7m7c7+4(L1+L2)c6K0+L7^{2}m7c_2q7)+2L7m7(2L3+L7c7)s5s6s7)+8I
y7dtdq3s7(s3c6c7+c3K10)+8Iy7c7(-dtdq7+c6K29+(dtdq2c3+dtdq5)
s6)(c3c6c7-3K10)+4K0s3(s5(dtdq4c6-dtdq6s6K5)+c5c6dtdq5(L3+q4))
+4L3m6s3c5(-tdq2K4+dtdq3s5s+dtdq5c6)K5+2dtdq3c3s5(4Iy6+L3^{2}m6
+2L3K5m6c6+(2L3+2K5c6+L7c7)L3m7)-dtdq3L3m7L7K14s7
+2c7dtdq3(-(4Iy7+L7^{2}m7)(s3c6s7+c3K24)+2c3s5L7m7(L3+K5c6))
+4m7s3s5(L3+K5)(2dtdq1K4+(K14L7s7+2K5s3s5s6)dtdq2-(L7s5c6s7-
2K5c5s6)dtdq3+dtdq42c6+L7s7(dtdq5s6-tdq7))+2(s3s5c7
+K4s7)(2L7m7(K4dtdq1+dtdq4c6+dtdq3c5s6K5+dtdq2s3s5s6K5)+(4Iy7
+L7^{2}m7)dtdq2s7(-1+s6-s5c6+K3))+8m6c6s3s5K5K2
+6s6s74m7(s3K5K6+L3c7K3)((2L3c7+L7)(dtdq3s5s6+dtdq5c6)+2K5dtdq
3c5c6s7-2dtdq1s7K3-
2dtdq4+dtdq2((c3c6+s3c5s6)(L7+2L3c7)+2s3K5s5c6s7))
+2K3(-17(dtdq3s5s6+dtdq5c6)-2L7m7s7(dtdq3c5c6K5-s6dtdq4)
+2L7m7dtdq1K3s7-dtdq2(K17K4+2K5L7m7s3s5c6s7))+s3s5(-
2(2L3+L7c7)L7m7dtdq7s7+4L3m6(dtdq1K4+c6dtdq4+S6K5K16))+8m6s

3s5s6K5(-c6(dtdq3c5K5+s3(-c5dtdq1+dtdq2s5K5))+s6(dtdq1c3
+dtdq4))+8(K5s3K25-K3L3s7)(L3m7(c7(K16+dtdq6)+(dtdq2
+dtdq3s5s6K4+dtdq5c6)s7)+m7c7(-(L2c6+L3)K16+dtdq4s6+(L1+L3
+q4)(c6K16-dtdq3c5c6)+dtdq1K3))),

$C_{63}(q,\dot{q}) =$ 1/8(+dtdq4K0c5c6-2dtdq5s5(4Iy6+L3^{2}m6+2L2L3m6c6+2L1L3m6c6)
+8s5Ix6(dtdq5+dtdq2c3)+2L7m7s5c6dtdq6s7(2L3+L7c7)+2s5L3L3m6(dt
dq2K4c6+dtdq3s5s6c6+dtdq5c6c6)+dtdq7s5(8Iy7s6+L7^{2}m7s6+4L3L7m
7s6c7+L7^{2}m7s6c_2q7)-8Iy7(c7K20(dtdq2K3+dtdq7-dtdq3s5c6))
+dtdq5(K10s7-K7s6c7))-2dtdq5((2(L1+L2)c6+2L3
+L7c7)(L7c7+2)L3m7s5-(c74Iy7K24+c5s6s7L7m7(2L3+L7c7)-s5c6
K0(L3+q4)))-4dtdq6c5s6K0K5+4L3m6s5K5K28+4m7c5(L3
+K5c6)(2s6K5K16+2dtdq1K4-tdq7s7L7+K3s7L7dtdq2+2dtdq4c6-
7dtdq3s5c6s7+L7dtdq5s6s7)+2K6(2L7m7(K4dtdq1+dtdq4c6)+2K5L7m7
K16s6-(4Iy7+L7^{2}m7)s7(K3dtdq2+dtdq7+s5c6dtdq3+dtdq5s6))
+8m6c5c6K5K26+4m7(L3s5c6c7-(L1+L2+L3)K24+K7)((2L3c7+L7)K28
+2(dtdq3K5c5c6s7-dtdq1K3s7+dtdq2s3s5c6s7K5-dtdq4s6s7))
+2s5c6(K17(dtdq3s5s6+dtdq5c6)+2dtdq3(L1+L2+L3)L7m7c5c6s7
-L7m7s7(dtdq1K3+dtdq4s6+c5c6dtdq3)+dtdq2(K4K17
+2K5L7m7s3c6s5s7))-c5(dtdq7L7m7s7(2L3+L7c7)-2L3m6K26)
+8m6c5s6K5(dtdq1K3+dtdq4s6-c6(dtdq2s3s5(L1+L2+L3)
+dtdq3c5K5))+8(K5K10+L3c6s5s7)(L3m7((-s6s7+c7)(K16+dtdq6)
+(c6(dtdq2c3+dtdq5))s7)+m7c7(-(L2c6+L3)K16-L3dtdq6
+(dtdq1c3+dtdq4)s6+(s3c5dtdq1-K16(L1+L3))c6))),

$C_{64}(q,\dot{q}) =$ 1/2(-c6K0dtdq6-L7m7(dtdq2c3s7+dtdq5s7-
tdq7s6s7)+2(m6+m7)(dtdq1s3c5-dtdq2s3s5K5-dtdq3c5K5)),

$C_{65}(q,\dot{q}) =$ 1/32(8dtdq7L7m7c6(2L3c7+L7c_2q7)+(K29)(32Ix6+16Ix7+16Iy7+4L3L3(
m6+4m7)-2c_2q6K8-2(L7+8L3)L7m7c_2q6c_2q6+2L7m7(3L7-
L7c_2q7+8L3c7))+2L7m7s7(2dtdq1c3+2dtdq4-(2L3+L7c7)dtdq6s6)-
K22(4dtdq2c3+dtdq5)s6c6),

$C_{66}(q,\dot{q}) =$ 1/4(2L3+L7c7)L7m7s7(K3dtdq2-s5c6dtdq3+dtdq5s6-
tdq7)+1/4K0(2dtdq1K4+2c6dtdq4+2K5K16s6),

$C_{67}(q,\dot{q}) =$ 1/4(dtdq3((4Ix7+L7^{2}m7+2L3L7m7)s5s6c7+2K5L7m7c5c6s7)+c6K17dtdq
5-L7m7s7(dtdq1K3+dtdq4s6)+dtdq2(K4K17+2s3K5L7m7c6s5s7)),

$C_{71}(q,\dot{q}) =$ 1/2m7(-L7dtdq7(c7K4-s3s5s7)-L7dtdq3(c3s5c7-(s3c6+c3s6s7)s7)
+L7dtdq6K3s7-L7s3K6dtdq5+L7K3(c7(dtdq2K4+dtdq3s5s6-dtdq5c6)
+(K16+dtdq6)s7)+2(c3c6c7-s3K10)((s7+c7)(dtdq1s3s5
+dtdq2(L3K3+s3c5K5)-dtdq3s5(K5+c6L3)+dtdq5s6L3)+(s7-c7)K26)),

$C_{72}(q,\dot{q}) =$ 1/4(-2L7m7dtdq4s3K6+K17dtdq3s3s6-dtdq6(K17K4
+2L7m7K5s3s5c6s7)+2L7m7dtdq7(K3L3s7+K20K5s3)+4((c6(dtdq2c3+dt
dq5)-(K29)s6)+K16+dtdq6)((Iy7+L7L7m7/4)(s3s5c7+K4s7)c7
+Iy7(c3c6c7-3K10)s7)+dtdq5s3(c6K17s5+2K5L7m7K7)+2L7m7s3s5(L3
+K5c6)(-7(c6(dtdq2c3+dtdq5)+(-c5dtdq2s3+dtdq3s5)s6)
+(K16+dtdq6)s7)-dtdq3c3(c5(2K5L7m7c7+c6K17)+2K5L7m7s5s6s7)
-4m7K3L3(K25s7s7+K26c7c7)-m7L7K3c7K26
+4m7K5K25s3s7(K25+K27L3)+K27(1+L3)(4m7K5K25s3c7+2m7L7K3s7)
+4m7s3K5K25(-c7K26+s7(dtdq2s3c5K5+s5(dtdq1s3-dtdq3K5)))),

$C_{73}(q,\dot{q}) =$ 1/2(L7m7dtdq4K7+(1/2c5c6(K17+2L3L7m7c7)+K5dtdq5K6)dtdq5-
1/2K17s5s6+L7m7c5c6s7K5)dtdq6-L7m7dtdq7(K10K5+L3s5c6s7)-
2((Iy7+L7L7m7/4)K6c7+Iy7K20s7)(c6(dtdq5+dtdq2c3)+(-
tdq2s3c5+dtdq3s5)s6)+2((Iy7+L7L7m7/4)K6s7-2Iy7K20c7)(K16+dtdq6)
+L7m7c5(-7(dtdq2K4+dtdq5c6)-tdq3K20+(dtdq2s3s5s7+dtdq6s7))(L3
+K5c6)+2m7(K5K10+L3c6s5s7)((L3c7-L3s7)K27+(s7+c7)K26+c7(dtdq2
K5s3c5+s5(dtdq1s3-dtdq3K5)))-2m7K5c5s6s7-(L7m7+28L3c7)
c6s5)(L3s7K27-c7K26+s7(dtdq2K5s3c5+s5(dtdq1s3-dtdq3K5)))),

$C_{74}(q,\dot{q}) =$ 1/4m7(-2L7c6dtdq7c7+4dtdq1s3s5c6-4K5s5c6dtdq3+2dtdq3s6(
2s5s6L3-5s7L7)+(2L3+L7c7)dtdq5s_2q6+dtdq2((2L3+4K5c6+2L3c_2q6-
L7(c7-c_2q6c_2q6))s3c5+4L3s6c3c6+2L7s6(c3c6c7-s3s5s7))),

$C_{75}(q,\dot{q}) =$ -1/4c6K17dtdq6+1/2L3L7m7dtdq7s6s7+((Iy7+L7L7m7/4)s7+Iy7c7)c6
+(-c7(c6(dtdq5+dtdq2c3)+(-dtdq2s3c5+dtdq3s5)s6)+(K16+dtdq6)s7)

+1/2L7m7s6s7(s3s5dtdq1+dtdq2(L3K3+s3c5K5)-dtdq3(K5s5+L3s5c6)
+dtdq5L3s6)-(2L3L3s6s7+1/2L7s6)K26m7c7,

$C_{76}(q,\dot{q}) =$ -(Iy7+1/2L3L7m7c7+L7L7m7/4c7c7)K28+(1/2L3L7m7
+L7L7m7/4)s7c7(K16+dtdq6),

$C_{77}(q,\dot{q}) =$ 1/2L7m7(-L3K27s7+c7K26+s7(K29K5+dtdq1s3s5)).